

Walls in supersymmetric massive nonlinear sigma model on complex quadric surface

Masato Arai^{†a}, Sunggeun Lee^{†b} and Sunyoung Shin^{‡c}

^{†#} *Center for Quantum Spacetime (CQUeST), Sogang University,
Shinsu-dong 1, Mapo-gu, Seoul 121-742, Korea*

[‡] *Department of Physics and Research Institute for Basic Sciences,
Kyung Hee University, Seoul 130-701, Korea*

[‡] *Department of Physics, Sungkyunkwan University,
Chunchun-dong 300, Jangan-gu, Suwon 440-746, Korea*

Abstract

The Bogomol'nyi-Prasad-Sommerfield (BPS) multiwall solutions are constructed in a massive Kähler nonlinear sigma model on the complex quadric surface, $Q^N = \frac{SO(N+2)}{SO(N) \times SO(2)}$ in 3-dimensional space-time. The theory has a nontrivial scalar potential generated by the Scherk-Schwarz dimensional reduction from the massless nonlinear sigma model on Q^N in 4-dimensional space-time and it gives rise to $2[N/2 + 1]$ discrete vacua. The BPS wall solutions connecting these vacua are obtained based on the moduli matrix approach. It is also shown that the moduli space of the BPS wall solutions is the complex quadric surface Q^N .

^aarai(at)sogang.ac.kr

^bsglkorea(at)hotmail.com

^csihnsy(at)skku.edu

1 Introduction

It is well known that topological solitons play an important role in various fields in physics such as string theory, field theory, cosmology and condensed matter physics. For the investigation of topological solitons supersymmetric (SUSY) field theories provide a nice arena since partial preservation of SUSY automatically gives the solution of equation of motion [1]. This solution is called the Bogomol'nyi-Prasad-Sommerfield (BPS) state [2]. One of the simplest BPS states is the so-called domain wall [3, 4], which is an extended object with codimension one. Since it preserves half of the original SUSY, it is called a half BPS state. Such a solution has been well studied in various SUSY models.

In particular, recently there has been progress in constructing wall solutions in SUSY gauge theories with eight supercharges in four and five dimensions [5, 6].⁴ In [5, 6] SUSY $U(N_C)$ gauge theory coupled to $N_F (> N_C)$ massive flavors with the Fayet-Iliopoulos term has been considered and a systematic way to construct possible BPS domain walls has been formulated. This formulation is called the moduli matrix approach. The mass term gives rise to a nontrivial scalar potential, yielding ${}_{N_F}C_{N_C}$ number of discrete vacua. Exact BPS multiwall solutions which interpolate these vacua with generic parameters covering the complete moduli space is obtained by taking the infinite gauge coupling. For certain values for the finite gauge coupling limit, exact BPS multiwall solutions are also obtained. It has been shown that the total moduli space of the BPS wall solutions is the Grassmann manifold, $G_{N_F, N_C} \equiv \frac{U(N_F)}{U(N_C) \times U(N_F - N_C)}$. The infinite gauge coupling limit yields vanishing kinetic terms of gauge fields and their superpartners. These fields just become Lagrange multipliers giving constraints to matter fields. In other words, the model becomes a quotient action of the massive hyper-Kähler (HK) nonlinear sigma model (NLSM) whose target metric is the cotangent bundle over the Grassmannian, $T^*G_{N_F, N_C}$. This model was originally studied in [12]. The same number of discrete vacua was obtained there but the BPS wall solutions were not. They were only known in massive HK NLSMs in the subclass of $T^*G_{N_F, N_C}$, especially, for $T^*G_{2,1} \simeq T^*\mathbf{C}P^1$ [4, 13, 14, 15, 16] until [5] appeared.

⁴By using the moduli matrix approach, various kinds of interesting solutions such as monopole-vortex-wall systems [7], domain wall webs [8], non-Abelian vortices [9], instanton-vortex systems [10] and Skyrmions [11] were also found in $U(N_C)$ gauge theories. For a comprehensive review, see [6].

The Grassmann manifold is one of the compact Hermitian symmetric spaces (HSS). The compact HSS consists of the four classical types

$$G_{N+M,M} = \frac{U(N+M)}{U(N) \times U(M)}, \quad \frac{SO(2N)}{U(N)}, \quad \frac{Sp(N)}{U(N)}, \quad Q^N = \frac{SO(N+2)}{SO(N) \times SO(2)}, \quad (1.1)$$

and the two exceptional types

$$\frac{E_6}{SO(10) \times U(1)}, \quad \frac{E_7}{E_6 \times U(1)}. \quad (1.2)$$

It would be interesting to investigate domain walls in massive HK NLSMs on cotangent bundles over the HSSs other than the Grassmann manifold. It is expected that they also possess discrete vacua and various kinds of domain walls connecting them. The moduli matrix approach would help to construct domain wall solutions in these models. In order to apply this approach to the above models, they have to be described as a quotient action, namely, SUSY gauge theories with infinite gauge coupling limit. Massless HK NLSMs on the cotangent bundles over the classical HSSs [17, 18, 19]⁵ and over the $\frac{E_6}{SO(10) \times U(1)}$ [21] were obtained in projective superspace [22, 23], but without using a gauge field Lagrange multiplier. Actually, it is difficult to construct them as a quotient action.

On the other hand, it was observed that when considering vacua and domain walls in the massive HK NLSM on $T^*G_{N_F, N_C}$, the cotangent part is irrelevant [15, 5]. In other words, in order to investigate them in this model, we can simply set the cotangent part to be zero. In this setting, the massive HK NLSM on $T^*G_{N_F, N_C}$ reduces to the massive Kähler NLSMs on G_{N_F, N_C} . The same situation would happen when considering massive HK NLSMs on cotangent bundles over HSSs other than G_{N_F, N_C} .⁶

Inspired by this observation, in this paper, we study a massive Kähler NLSM on the complex quadric surface, $Q^N = \frac{SO(N+2)}{SO(N) \times SO(2)}$. We start with the massless Kähler NLSM on Q^N in 4-dimensional space-time which has been formulated as a SUSY gauge theory in [25]. Its massive

⁵A massless HK NLSM on the tangent bundle over the complex quadric surface being one of the classical HSSs has been worked out in [20].

⁶For the case of the HSS \mathcal{M} , it is expected that the moduli space of domain walls is the base manifold \mathcal{M} as in the case of the $T^*G_{N,M}$ model. However, the moduli space of walls is not \mathcal{M} in general. Such an example has been examined in the NLSM on $T^*\mathcal{M}$ where \mathcal{M} is a special Lagrangian submanifold [24].

version can be constructed via the Scherk-Schwarz dimensional reduction [26]. Mass terms are characterized by the Cartan matrix of the isometry of the model, $SO(N+2)$ and give rise to a nontrivial scalar potential. From the vacuum condition we find that the theory has $2 \left[\frac{N}{2} + 1 \right]$ discrete vacua. We also find the exact domain wall solutions interpolating these vacua and the moduli spaces of the solutions. The latter is shown to be the complex quadric surface.

Organization of this paper is as follows. In Section 2, we introduce our model and investigate vacuum structure. We also derive half BPS equations. In Section 3, exact solutions of the BPS equations are obtained in the use of the moduli matrix approach. Section 4 is devoted to conclusion and discussion. In Appendix A, we list moduli matrices of multiwalls including compressed walls for the $N = 4$ case. In Appendix B, possible parameter regions for a quadruple wall in the $N = 4$ case are given.

2 Massive Kähler NLSM on Q^N

We start with a brief review of the massless NLSM on Q^N in 4-dimensional space-time. We basically follow the notation of [27].

The SUSY gauge theory realizing the NLSM on Q^N in terms of the $\mathcal{N} = 1$ superfields in 4-dimensional space-time is given in [25]. Let $\phi^i(x, \theta, \bar{\theta})$ ($i = 1, \dots, N+2$) be chiral superfields, $\bar{D}_{\dot{\alpha}} \phi^i = 0$ belonging to a vector representation of $SO(N+2)$. Introducing an auxiliary vector superfield $V(x, \theta, \bar{\theta})$ ($= V^\dagger$) and an auxiliary chiral superfield $\phi_0(x, \theta, \bar{\theta})$, being a singlet representation of $SO(N+2)$, the Lagrangian is described as

$$\mathcal{L} = \int d^4\theta (\bar{\phi}^i \phi^i e^V - r^2 V) + \left(\int d^2\theta \phi_0 (\phi^i)^2 + \text{c.c.} \right), \quad (2.1)$$

where r^2 is a real positive constant called the Fayet-Iliopoulos parameter. Repeated indices i are summed over here. In the following this rule is implicitly assumed unless stated. This Lagrangian possesses gauge invariance

$$V \rightarrow V - \Lambda - \Lambda^\dagger, \quad \phi^i \rightarrow e^\Lambda \phi^i, \quad \phi_0 \rightarrow e^{-2\Lambda} \phi_0, \quad (2.2)$$

with an arbitrary chiral superfield $\Lambda(x, \theta, \bar{\theta})$. The equation of motion for V is given by $\bar{\phi}^i \phi^i e^V - r^2 = 0$, which can be solved as $V = -\log(\bar{\phi}^i \phi^i / r^2)$. If the superpotential is absent in the

Lagrangian (2.1), we obtain the Kähler potential of $\mathbf{C}P^{N+1}$. In this case, substituting the solution back into the Kähler potential of (2.1), we have

$$K = r^2 \log \left(1 + \frac{\bar{\Phi}^a \Phi^a}{r^2} \right), \quad (2.3)$$

with a gauge fixing $\phi^T = (\Phi^a, r) (a = 1, \dots, N+1)$. The superpotential in (2.1) gives an additional constraint through the equation of motion for ϕ_0 :

$$(\phi^i)^2 = 0. \quad (2.4)$$

Therefore, the complex quadric surface is defined as a hypersurface embedded into the complex projective plane $\mathbf{C}P^{N+1}$ [28, 29]. Let us solve the constraint (2.4). First, we decompose ϕ^i into a representation of a $SO(N) \times U(1)$ group of $SO(N+2)$ as $\phi^T = (x, y^I, z)$ where x and z are complex scalars, and $y^I (I = 1, \dots, N)$ is a complex vector. Performing the unitary transformation [25]

$$\phi \rightarrow \begin{pmatrix} \frac{i}{\sqrt{2}} & 0 & \frac{1}{\sqrt{2}} \\ 0 & \mathbf{1}_N & 0 \\ -\frac{i}{\sqrt{2}} & 0 & \frac{1}{\sqrt{2}} \end{pmatrix} \phi, \quad (2.5)$$

then (2.4) becomes

$$(\phi^i)^2 \rightarrow \phi^T J \phi = 2xz + (y^I)^2 = 0. \quad (2.6)$$

Here J is the rank 2 invariant tensor defined as

$$J = \begin{pmatrix} 0 & \mathbf{0} & 1 \\ \mathbf{0} & \mathbf{1}_n & \mathbf{0} \\ 1 & \mathbf{0} & 0 \end{pmatrix}. \quad (2.7)$$

The constraint (2.6) can be solved to give $\phi^T = (x, y^I, -\frac{(y^I)^2}{2x})$. Eliminating V and making a gauge fixing as $\phi^T = (r, \Phi^I, -\frac{(\Phi^I)^2}{2})$, we obtain the Kähler potential of the quadric surface [30, 31, 32]

$$K = r^2 \log \left(1 + \frac{\bar{\Phi}^I \Phi^I}{r^2} + \frac{(\Phi^I)^2 (\bar{\Phi}^I)^2}{4r^2} \right). \quad (2.8)$$

Next we derive a massive NLSM on Q^N . In the above, starting from the quotient action, we eliminate the vector superfield V and make a gauge fixing to obtain the known Kähler potential. In order to utilize the formulation in [5, 6] we leave the vector superfield in the action as an independent degree of freedom. Since we are interested in a solitonic solution, we focus only on the bosonic part of the Lagrangian in the following. Substituting the expressions

$$\begin{aligned}\phi^i(x, \theta, \bar{\theta}) &= \phi^i(x) + \theta^2 F^i, \\ \phi_0(x, \theta, \bar{\theta}) &= \phi_0(x) + \theta^2 F_0, \\ V(x, \theta, \bar{\theta}) &= 2\theta\sigma^\mu\bar{\theta}v_\mu + \frac{1}{2}\theta^2\bar{\theta}^2 D,\end{aligned}\tag{2.9}$$

into (2.1), the bosonic part of the Lagrangian becomes (we take $r = 1$ for simplicity)

$$\begin{aligned}\mathcal{L}_{\text{bos}} &= -\partial_\mu\phi^i\partial^\mu\bar{\phi}^i + |F^i|^2 - iv_\mu(\bar{\phi}^i\partial^\mu\phi^i - \partial^\mu\bar{\phi}^i\phi^i) - v^\mu v_\mu\bar{\phi}^i\phi^i + \frac{1}{2}D(\bar{\phi}^i\phi^i - 1) \\ &\quad + F_0(\phi^i)^2 + \bar{F}_0(\bar{\phi}^i)^2 + 2\phi_0\phi^i F^i + 2\bar{\phi}_0\bar{\phi}^i \bar{F}^i.\end{aligned}\tag{2.10}$$

The Greek letter μ denotes a 4-dimensional space-time index. Eliminating the auxiliary fields, we obtain the scalar potential

$$V = |F^i|^2 = 4|\phi_0|^2|\phi^i|^2,\tag{2.11}$$

and the constraints

$$(\phi^i)^2 = 0, \quad (\bar{\phi}^i)^2 = 0, \quad |\phi^i|^2 - 1 = 0.\tag{2.12}$$

The vacuum condition $V = 0$ tells us that $\phi_0 = 0$ or $\phi^i = 0$. The latter is inconsistent with the last condition in (2.12) while the former solution is consistent and leads to $\phi^i \neq 0$. However, the former one does not give discrete vacua. Therefore, no domain wall solution exists in this case.

The situation changes when mass terms are introduced in the above model. We perform the Scherk-Schwarz dimensional reduction for the generation of mass [26]. Specifying that fields in the x^3 direction move along orbits of the Killing vectors $f(\phi)$ and $\bar{f}(\bar{\phi})$ in the quadric surface

$$\frac{\partial\phi^i}{\partial x^3} = f^i(\phi) = -iM^{ij}\phi^j, \quad \frac{\partial\bar{\phi}^i}{\partial x^3} = \bar{f}^i(\bar{\phi}) = i(M^{ij}\phi^j)^\dagger,\tag{2.13}$$

where M^{ij} is the Cartan matrices of $SO(N+2)$ given by

$$M^{ij} = \sum_{a=1}^{[\frac{N}{2}+1]} m_a \delta_{aa} \otimes \sigma_2 \quad (\text{even } N), \quad (2.14)$$

$$M^{ij} = \begin{pmatrix} \sum_{a=1}^{[N/2+1]} m_a \delta_{aa} \otimes \sigma_2 & 0 \\ 0 & 0 \end{pmatrix} \quad (\text{odd } N). \quad (2.15)$$

Here m_a is a real mass parameter and δ_{aa} is the $[N/2+1] \times [N/2+1]$ unit matrix. The matrix M^{ij} can be generic if we take $m_a \neq 0$ for every a and $m_a^2 \neq m_b^2$ for $a \neq b$. In this paper, we further assume that $m_a > m_{a+1} > 0$. Note that by introducing mass terms, flavor symmetry $SO(N+2)$ is broken down to $SO(2)^{[N/2+1]}$.

Substituting (2.13) into the component action (2.10), we have

$$\begin{aligned} \mathcal{L}_{\text{bos}} = & -\partial^m \bar{\phi}^i \partial_m \phi^i - |f^i|^2 + |F^i|^2 - iv_m (\bar{\phi}^i \partial^m \phi^i - \partial^m \bar{\phi}^i \phi^i) - i\sigma (\bar{\phi}^i f^i(\phi) - \bar{f}^i(\bar{\phi}) \phi^i) \\ & -(v^m v_m + \sigma^2) \bar{\phi}^i \phi^i + \frac{1}{2} D (\bar{\phi}^i \phi^i - 1) \\ & + F_0 (\phi^i)^2 + \bar{F}_0 (\bar{\phi}^i)^2 + 2\phi_0 \phi^i F^i + 2\bar{\phi}_0 \bar{\phi}^i \bar{F}^i, \end{aligned} \quad (2.16)$$

where $\sigma = v_3$. A Roman letter index m refers to the first three components of the 4-dimensional index μ . Eliminating the auxiliary fields F^i, F_0 and D , we have

$$\mathcal{L}_{\text{bos}} = -\partial_m \phi^i \partial^m \bar{\phi}^i - iv_m (\bar{\phi}^i \partial^m \phi^i - \partial^m \bar{\phi}^i \phi^i) - v^m v_m \bar{\phi}^i \phi^i - V, \quad (2.17)$$

with the constraints (2.12). The scalar potential V is given by

$$V = |f^i - i\sigma \phi^i|^2 + 4|\phi_0|^2 |\phi^i|^2. \quad (2.18)$$

The first term comes from the dimensional reduction and it gives rise to discrete vacua as we will see below. The vacuum condition is readily read off as

$$f^i(\phi) - i\sigma \phi^i = 0, \quad (2.19)$$

and

$$\phi_0 = 0 \quad \text{or} \quad \phi^i = 0, \quad (2.20)$$

with the constraints (2.12). The latter solution in (2.20) is inconsistent with the last constraints in (2.12). Therefore, we shall consider the case, $\phi_0 = 0$ and $\phi^i \neq 0$. The condition (2.19) is rewritten by

$$0 = |f^i(\phi) - i\sigma\phi^i|^2 = (\bar{\phi}^{2a-1}, \bar{\phi}^{2a}) \begin{pmatrix} \sigma & im_a \\ -im_a & \sigma \end{pmatrix}^2 \begin{pmatrix} \phi^{2a-1} \\ \phi^{2a} \end{pmatrix} + c|\sigma\phi^{N+2}|^2, \quad (2.21)$$

where a is the flavor index running from 1 to $[N/2 + 1]$ and c takes 0 for even N cases and 1 for odd N cases. For later convenience, we perform the unitary transformation (it makes the Bogomol'nyi completion of the Hamiltonian easy as will be seen in the next section)

$$\begin{pmatrix} \phi^{2a-1} \\ \phi^{2a} \end{pmatrix} \rightarrow \Phi^{\alpha a} \equiv \begin{pmatrix} \Phi^{1a} \\ \Phi^{2a} \end{pmatrix} = \frac{1}{\sqrt{2}} \begin{pmatrix} 1 & -i \\ 1 & i \end{pmatrix} \begin{pmatrix} \phi^{2a-1} \\ \phi^{2a} \end{pmatrix}, \quad (2.22)$$

where $\alpha = 1, 2$. Equation (2.21) is rewritten by

$$0 = \sum_{i=1}^{[\frac{N}{2}+1]} \sum_{\alpha=1}^2 |\lambda_{\alpha a} \Phi^{\alpha a}|^2 + c|\sigma\phi^{N+2}|^2, \quad \lambda_{\alpha a} \in \mathbf{R}, \quad (2.23)$$

where $\lambda_{1a} = \sigma + m_a$ and $\lambda_{2a} = \sigma - m_a$. The constraints (2.12) become

$$|\Phi^{\alpha a}|^2 + c|\phi^{N+2}|^2 = 1, \quad (2.24)$$

$$2\Phi^{1a}\Phi^{2a} + c(\phi^{N+2})^2 = 0 \quad \text{and c.c.} \quad (2.25)$$

In the following, we solve the set of these equations for even and odd N cases, separately.

a) Even N case

In this case, Equation (2.23) tells us that

$$\lambda_{\alpha a} \Phi^{\alpha a} = 0. \quad (\text{no sum for } \alpha, a) \quad (2.26)$$

Equation (2.26) leads to $\lambda_{\alpha a} = 0$ or $\Phi^{\alpha a} = 0$. Among them the former one is only consistent with (2.24). It gives two solutions $\sigma = -m_a$ and $\sigma = m_a$. The first case says that $\Phi^{1a} \neq 0$ and $\Phi^{2a} = 0$ for some a . The constraint (2.25) is satisfied with this solution while (2.24) gives $|\Phi^{\alpha a}|^2 = 1$. Therefore, a solution in this case is

$$\Phi^{\alpha a} = \begin{pmatrix} 0 & \cdots & 0 & 1 & 0 & \cdots & 0 \\ 0 & \cdots & 0 & 0 & 0 & \cdots & 0 \end{pmatrix}, \quad \sigma = -m_a, \quad (2.27)$$

where a phase is set to be zero by the flavor symmetry $SO(2)^{[N/2+1]}$. There exist $[N/2 + 1]$ solutions as the index runs from 1 to $[N/2 + 1]$. Similarly we can analyze for the second case $\sigma = m_a$. A solution for some a is given by

$$\Phi^{\alpha a} = \begin{pmatrix} 0 & \cdots & 0 & 0 & 0 & \cdots & 0 \\ 0 & \cdots & 0 & 1 & 0 & \cdots & 0 \end{pmatrix}, \quad \sigma = m_a. \quad (2.28)$$

Again we see that there are $[N/2 + 1]$ solutions. Taking into account both cases, we find that the theory has $2[N/2 + 1]$ vacuum solutions.

b) Odd N case

In this case, the vacuum condition is given by

$$\sigma \phi^{N+2} = 0, \quad (2.29)$$

in addition to (2.26). From (2.29), we have $\sigma = 0$ or $\phi^{N+2} = 0$. The former solution with (2.26) leads to $\Phi^{\alpha a} = 0$ and $|\phi^{N+2}|^2 = 1$. This is inconsistent with (2.25). It is therefore not a solution. Considering the $\phi^{N+2} = 0$ case, the situation turns out to be the same as the even N case. Therefore, we find that there exist $2[N/2 + 1]$ vacuum solutions for the odd N case.

We make comments in order. For the $N = 1$ case, the target metric of our model is Q^1 which is isomorphic to \mathbf{CP}^1 and the theory has two discrete vacua. This number of vacua is the same with one in the massive $T^*\mathbf{CP}^1$ NLSM model [15]. As mentioned in the Introduction, the cotangent part of the massive $T^*\mathbf{CP}^1$ model is irrelevant when considering vacua and wall solutions. Therefore, we find that our vacuum solution for the $N = 1$ case is consistent with the result of the massive $T^*\mathbf{CP}^1$ model. For the $N = 4$ case, the target space becomes Q^4 which is isomorphic to Grassmannian, $G_{4,2}$. In this case, there exist six vacua. On the other hand, it is known that there are ${}_{N_F}C_{N_C}$ vacuum solutions in the massive NLSM on $T^*G_{N_F, N_C}$ [12], yielding six vacua for the $T^*G_{4,2}$ case. Repeating the same discussion as in the $N = 1$ case we again find that our result is consistent. New results appear in other cases. For instance, for the $N = 2$ and $N = 3$ cases, target spaces of our model are isomorphic to $\mathbf{CP}^1 \times \mathbf{CP}^1$ and $Sp(2)/U(2)$, respectively. There exist four vacua in both cases. For $N > 4$, there is no isomorphism and this is therefore purely the result of the complex quadric surface.

3 BPS equations

In this section, we derive the BPS equation through the Bogomol'nyi completion of (the bosonic part of) the Hamiltonian. Since we are interested in a time-independent wall solution, we assume that fields have no time dependence, $\partial_0\phi^i = 0$ and that all fields depend on the coordinate of only one dimension of x_1 , which we shall write x . We also assume the Poincaré invariance on the two-dimensional world volume of the wall, which implies $v_0 = v_2 = 0$. The energy along the x direction is given by

$$\begin{aligned}
E &= \int dx (|D_1\phi^i|^2 + |f^i - i\sigma\phi^i|^2 + 4|\sigma\phi_0|^2) \\
&= \int dx \left\{ \sum_{a=1}^{[\frac{N}{2}+1]} \sum_{\alpha=1}^2 (|D_1\Phi^{\alpha a}|^2 + |\lambda_{\alpha a}\Phi^{\alpha a}|^2 + 4|\phi_0\Phi^{\alpha a}|^2) \right. \\
&\quad \left. + c(|D_1\phi^{N+2}|^2 + \sigma^2|\phi^{N+2}|^2 + 4|\phi_0\phi^{N+2}|^2) \right\}, \tag{3.1}
\end{aligned}$$

with the constraints (2.24) and (2.25). The covariant derivative is defined by $D_1\Phi^{\alpha a} = (\partial_1 - iw_1)\Phi^{\alpha a}$. The Bogomol'nyi completion of the energy can be performed as

$$\begin{aligned}
E &= \int dx \left\{ \sum_{a=1}^{[\frac{N}{2}+1]} \sum_{\alpha=1}^2 (|D_1\Phi^{\alpha a} \mp \lambda_{\alpha a}\Phi^{\alpha a}|^2 + 4|\phi_0\Phi^{\alpha a}|^2) \right. \\
&\quad \left. + c(|D_1\phi^{N+2} \mp \sigma\phi^{N+2}|^2 + 4|\phi_0\phi^{N+2}|^2) \pm T \right\} \geq \pm T, \tag{3.2}
\end{aligned}$$

where T is a tension defined by

$$T \equiv \int dx \sum_{a=1}^{[\frac{N}{2}+1]} \partial_1 m_a (|\Phi^{1a}|^2 - |\Phi^{2a}|^2). \tag{3.3}$$

From (3.2) the BPS equations are obtained as

$$D_1\Phi^{\alpha a} \mp \lambda_{\alpha a}\Phi^{\alpha a} = 0, \quad (\text{no sum for } \alpha, a) \tag{3.4}$$

$$\phi_0\Phi^{\alpha a} = 0, \tag{3.5}$$

$$D_1\phi^{N+2} \mp \sigma\phi^{N+2} = 0, \tag{3.6}$$

$$\phi_0\phi^{N+2} = 0. \tag{3.7}$$

Equations (3.5) and (3.7) tell us that $\phi_0 = 0$ or $\Phi^{\alpha a} = \phi^{N+2} = 0$, but the latter solution is inconsistent with (2.24). Taking the former solution, the BPS equations are simplified to be (here we take upper sign in (3.4) and (3.6))

$$D_1 \Phi^{\alpha a} - \lambda_{\alpha a} \Phi^{\alpha a} = 0, \quad (\text{no sum for } \alpha, a) \quad (3.8)$$

$$D_1 \phi^{N+2} - \sigma \phi^{N+2} = 0. \quad (3.9)$$

4 BPS wall solution

4.1 BPS equations

In this section we solve the BPS equations (3.8) and (3.9) together with the constraints (2.24) and (2.25) by using the moduli matrix approach [5, 6]. First of all, we introduce a complex function $S(x)$ defined by

$$-\sigma - iv_1 = S^{-1}(x) \partial_1 S(x). \quad (4.1)$$

Let us change variables from $\Phi^{\alpha a}$ and ϕ^{N+2} to complex valued functions $f^{\alpha a}$ and f^{N+2} by using S

$$\Phi^{\alpha a} \equiv S^{-1} f^{\alpha a}, \quad \phi^{N+2} \equiv S^{-1} f^{N+2}. \quad (4.2)$$

Substituting (4.1) and (4.2) into (3.8) and (3.9), we have

$$\partial_1 f^{\alpha a} = (\hat{M}_a)^\alpha_\beta f^{\beta a}, \quad \partial f^{N+2} = 0, \quad (\text{no sum for } a) \quad (4.3)$$

where $\hat{M}_a \equiv \text{diag}(m_a, -m_a)$. It can be easily solved as

$$f^{\alpha a} = (e^{\hat{M}_a x})^\alpha_\beta H_0^{\beta a}, \quad f^{N+2} = H_0^{N+2}, \quad (\text{no sum for } a) \quad (4.4)$$

with a complex constant matrix $H_0^{\alpha a}$ and a complex constant H_0^{N+2} as integration constants. Since they include information of vacua and positions of walls, it is called the moduli matrix [5, 6]. From (4.4), $\Phi^{\alpha a}$ and ϕ^{N+2} can be solved in terms of S as

$$\Phi^{\alpha a} = S^{-1} (e^{\hat{M}_a x})^\alpha_\beta H_0^{\beta a}, \quad \phi^{N+2} = S^{-1} H_0^{N+2}. \quad (\text{no sum for } a) \quad (4.5)$$

The definitions (4.1) and (4.2) show that a set (S, H_0) and another set (S', H'_0) give the same original fields σ , v_1 , $\Phi^{\alpha a}$, and ϕ^{N+2} , provided that they are related by

$$S' = VS, \quad H_0^{\alpha a'} = VH_0^{\alpha a}, \quad H_0^{N+1'} = VH_0^{N+1}, \quad (4.6)$$

where $V \in \mathbf{C}^* = \mathbf{C} - \{0\}$. This transformation V defines an equivalent class among sets of the functions $(S, H_0^{\alpha a}, H_0^{N+2})$ which represent physically equivalent results. This kind of symmetry is called the world-volume symmetry [5]. It is seen that the equivalence relation (4.6) with the constraints (2.24) and (2.25) defines the complex quadric surface. Making the unitary transformation,

$$\begin{pmatrix} H_0^{1a} \\ H_0^{2a} \end{pmatrix} \rightarrow \begin{pmatrix} H_0^{2a-1} \\ H_0^{2a} \end{pmatrix} = \frac{1}{\sqrt{2}} \begin{pmatrix} 1 & 1 \\ i & -i \end{pmatrix} \begin{pmatrix} H_0^{1a} \\ H_0^{2a} \end{pmatrix}, \quad (4.7)$$

and defining the vector $H_0^i \equiv (H_0^{2a-1}, H_0^{2a}, H_0^{N+2})$ ($i = 1, \dots, N+2$), then Eqs. (4.6), (2.24) and (2.25) are

$$S' = VS, \quad H_0^{i'} = VH_0^i, \quad (4.8)$$

$$|H_0^i|^2 = 1, \quad (H_0^i)^2 = 0, \quad (\bar{H}_0^i)^2 = 0. \quad (4.9)$$

This is nothing but the definition of the complex quadric surface [29]. Therefore, the moduli space of the domain walls is the complex quadric surface.

Since the BPS equation for matter parts are solved by means of the function S , the remaining task is to solve the constraints (2.24) and (2.25). Substituting (4.5) into (2.24) and (2.25), we have

$$H_{0\alpha}^\dagger{}^a (e^{2\hat{M}_a x})^\alpha{}_\beta H_0^{\beta a} + c |H_0^{N+2}|^2 = SS^\dagger, \quad (4.10)$$

$$2H_0^{1a} H_0^{2a} + c (H_0^{N+2})^2 = 0 \quad \text{and} \quad \text{c.c.} \quad (4.11)$$

Once a moduli matrix is given, S is also obtained by (4.10) and eventually the explicit solutions $\Phi^{\alpha a}$ and ϕ^{N+2} are obtained. A form of moduli matrix should be determined so that it includes information of vacua, boundary conditions and positions of walls. In addition, it must satisfy the constraint (4.11). In the next section, we show various types of possible moduli matrices and investigate their properties.

4.2 Properties of moduli matrix

a) Vacuum

This is the simplest example of the moduli matrix. For the even N case, the moduli matrices $H_0^{\alpha a}$ corresponding to vacua are given by

$$H_{0\langle k \rangle} = \begin{pmatrix} & & & \text{k-th} & & & \\ 0 & \cdots & 0 & 1 & 0 & \cdots & 0 \\ 0 & \cdots & 0 & 0 & 0 & \cdots & 0 \end{pmatrix}, \quad \sigma = -m_k, \quad (4.12)$$

or

$$H_{0\langle k \rangle} = \begin{pmatrix} & & & \text{k-th} & & & \\ 0 & \cdots & 0 & 0 & 0 & \cdots & 0 \\ 0 & \cdots & 0 & 1 & 0 & \cdots & 0 \end{pmatrix}, \quad \sigma = m_k, \quad (4.13)$$

where the index k in $H_{0\langle k \rangle}$ labels the k -th vacua. In what follows, we represent $\langle k \rangle$ as the k -th vacuum. These forms trivially satisfy (4.11). One can easily check that they yield the vacuum solutions (2.27) and (2.28). Substituting them into (4.10), we have

$$S_{\langle k \rangle} = e^{m_k x} \quad \text{for } \sigma = -m_k, \quad (4.14)$$

$$S_{\langle k \rangle} = e^{-m_k x} \quad \text{for } \sigma = m_k. \quad (4.15)$$

Here we take the phase to be zero by using the flavor symmetry $SO(2)$. Substituting (4.14) and (4.15) with (4.12) and (4.13) into (4.5), the vacuum solutions (2.27) and (2.28) are obtained.

For the odd N case, we just take into account $H_0^{N+2} = 0$ in addition to (4.12) and (4.13). Repeating the same analysis as was performed in the even N case, one can see that they satisfy the constraint (4.11) and give the correct vacua.

b) Single wall

A simple example of a nontrivial configuration is a wall configuration connecting two vacua, which we call a single wall. First we consider the even N case. In this case, a moduli matrix $H_0^{\alpha a}$ representing a single wall connecting two vacua is written by two nonzero components. For example, a moduli matrix satisfying (4.11) is given by

$$H_{0\langle k \leftarrow k+1 \rangle} = \begin{pmatrix} \dots & 0 & \overset{\text{k-th}}{e^{r_k}} & \overset{\text{k+1-th}}{e^{r_{k+1}}} & 0 & \dots \\ \dots & 0 & 0 & 0 & 0 & \dots \end{pmatrix}, \quad r_i \in \mathbf{C}, \quad (4.16)$$

where we parametrize nonzero factor by exponent with complex constants r_i ($i = k, k + 1$) for convenience⁷ and take one exponential factor to be a unit by using the world-volume symmetry transformation (4.6), namely, $r_k = 0$. Here the suffix $\langle k \leftarrow k + 1 \rangle$ denotes the moduli matrix describing the BPS state interpolating from the vacuum $\langle k + 1 \rangle$ at $x = -\infty$ to the vacuum $\langle k \rangle$ at $x = \infty$.

One can check that this moduli matrix gives the vacua at boundaries, $x = \pm\infty$. In order to see that, notice that the solution for $\Phi^{\alpha a}$ and ϕ^{N+2} in (4.5) implies the transformation of the moduli matrix

$$H_0^{\alpha a} \rightarrow (e^{\tilde{M}_a x_0})^\alpha_\beta H_0^{\beta a}, \quad H_0^{N+2} \rightarrow H_0^{N+2}, \quad (\text{no sum for } a) \quad (4.17)$$

under a translation $x \rightarrow x + x_0$. For the case of (4.16), we have

$$H_0^{1b} \rightarrow e^{m_b x_0} H_0^{1b}, \quad (b = k \text{ or } k + 1) \quad (4.18)$$

while H_0^{2a} remains to be zero. Since the world-volume symmetry transformation (4.6) allows us to multiply H_0^{1a} by the factor $V = e^{-m_k x_0 - r_k}$, we have

$$V H_0^{1a} = (\dots, 0, 1, \mathcal{O}(e^{-(m_k - m_{k+1})x_0}), 0, \dots). \quad (4.19)$$

Taking $x_0 \rightarrow \infty$, one sees that the moduli matrix becomes $H_{0\langle k \rangle}$ given by (4.12). Similarly, multiplying H_0^{1a} by $V = e^{-m_{k+1} x_0 - r_{k+1}}$ and taking $x_0 \rightarrow -\infty$, one sees that the moduli matrix becomes $H_{0\langle k+1 \rangle}$.

The following moduli matrix is also possible to express a single wall

$$H_{0\langle l-1 \leftarrow l \rangle} = \begin{pmatrix} \dots & 0 & 0 & 0 & 0 & \dots \\ \dots & 0 & \underset{\text{l-th}}{e^{r_l}} & \underset{\text{l-1-th}}{e^{r_{l-1}}} & 0 & \dots \end{pmatrix}. \quad (4.20)$$

⁷We follow the same parametrization as in [5].

Repeating the same analysis as in the previous case, it can be seen that the moduli matrix gives the vacua $\langle l \rangle$ and $\langle l - 1 \rangle$ at $x = -\infty$ and $x = \infty$, respectively. In this case the most left (right) nonzero component represents the vacuum at $x = -\infty$ ($x = \infty$) unlike the previous case because opposite signs of masses appear in the shift of H_0^{2a} according to (4.17).

Another possible choice for wall configurations is to take one nonzero component both in the first and the second lines in $H_0^{\alpha a}$, respectively. For example,

$$H_{0\langle k \leftarrow l \rangle} = \begin{pmatrix} \cdots & 0 & e^{r_k} & 0 & 0 & \cdots \\ \cdots & 0 & 0 & e^{r_l} & 0 & \cdots \end{pmatrix}, \quad (4.21)$$

which also satisfies (4.11). In this case, one can check that the vacuum $\langle k \rangle$ is at $x = \infty$ and the vacuum $\langle l \rangle$ is at $x = -\infty$.

The following moduli matrix is not allowed as a single wall configuration for the even N case

$$H_{0\langle k \leftarrow l \rangle} = \begin{pmatrix} \cdots & 0 & e^{r_k} & 0 & \cdots \\ \cdots & 0 & e^{r_l} & 0 & \cdots \end{pmatrix}, \quad (4.22)$$

since it does not satisfy the constraint (4.11).

Next we consider the odd N case. In this case, we just take into account H_0^{N+2} in (4.10) and (4.11). It is easy to see that configurations such as (4.16), (4.20) and (4.21) are possible with $H_0^{N+2} = 0$. In addition to these configurations, (4.22) is also allowed since (4.11) can be satisfied if H_0^{N+2} has the following values:

$$H_0^{N+2} = \sqrt{2}i e^{(r_k+r_l)/2}. \quad (4.23)$$

The nonzero value of H_0^{N+2} gives a nontrivial configuration of ϕ^{N+2} through (4.5). In this case, the moduli matrix (4.22) gives the vacuum $\langle k \rangle$ at $x = \infty$ and the vacuum $\langle l \rangle$ at $x = -\infty$ while H_0^{N+2} approaches 0 at both boundaries.

From the above observation, we can see that the most left nonzero component in the first line of $H_0^{\alpha a}$ represents a vacuum at $x = \infty$ while a vacuum represented by the most left nonzero component in the second line is at $x = -\infty$. It is also true for general (multiwall) cases:

$$H_{0\langle 1 \leftarrow k \rangle} = \begin{pmatrix} \cdots & 0 & e^{r_1} & * & \cdots \\ & 0 & \cdots & 0 & e^{r_k} & * & \cdots \end{pmatrix} \begin{matrix} \uparrow x \rightarrow \infty, \\ \text{1st} \quad x \rightarrow \infty \\ \leftarrow \\ \text{k-th} \quad x \rightarrow \infty \\ \rightarrow \end{matrix} \quad (4.24)$$

where the asterisk expresses either zero or nonzero components. We will show possible forms of multiwall configurations.

Before going to the discussion of multiwall configurations, we give some definitions concerning single walls. Single wall configurations are classified into two types. For even and odd N cases of the moduli matrix given by

$$H_{0\langle k \leftarrow l \rangle} = \begin{pmatrix} \cdots & 0 & e^{r_k} & \underbrace{0 \cdots 0}_n & e^{r_l} & 0 & \cdots \\ \cdots & 0 & 0 & \cdots & 0 & 0 & \cdots \end{pmatrix}, \quad (4.25)$$

this state defines an elementary wall or a compressed wall if $n = 0$ or $n \neq 0$, respectively [5]. Here n is called the level of the single wall. They appear in a different form of the moduli matrix which has a nonzero component in the first and the second lines in H_0^{aa} , respectively,

$$H_{0\langle k \leftarrow l \rangle} = \begin{pmatrix} \cdots & 0 & e^{r_k} & \underbrace{0 \cdots \cdots 0}_n \\ \cdots & 0 & \cdots & 0 & e^{r_l} & \underbrace{0 \cdots \cdots 0}_m \end{pmatrix}. \quad (4.26)$$

For the even (odd) N cases, the configuration represents an elementary wall or a compressed wall if $n + m = 1$ ($n + m = 0$) or $n + m > 1$ ($n + m > 0$), respectively. Compressed walls are obtained as compression of a multiwall configuration. We will see in detail through the explicit examples which will be explained in the next section.

c) Multiwalls

It is easy to extend above configurations into multiwalls interpolating discrete vacua. Let us consider the even N case first. A simple configuration connecting n vacua is given by, for example,

$$H_{0\langle 1 \leftarrow n \rangle} = \begin{pmatrix} \cdots & 0 & e^{r_1} & e^{r_2} & \cdots & e^{r_n} & 0 & \cdots \\ \cdots & 0 & 0 & 0 & \cdots & 0 & 0 & \cdots \end{pmatrix}, \quad n \leq N/2 + 1, \quad (4.27)$$

which trivially satisfies the constraint (4.11). In what follows we will show that this configuration interpolates multiple vacua. With the use of (4.17), H_0^{1a} transforms as

$$H_0^{1a} \rightarrow e^{m_a x_0} H_0^{1a}, \quad (\text{no sum for } a) \quad (4.28)$$

while H_0^{2a} remains to be zero. Multiplying H_0^{1a} by the factor $V = e^{-m_l x_0 - r_l}$, the vector $V H_0^{1a} e^{m_a x_0}$ becomes

$$V H_0^{1a} e^{m_a x_0} = (\dots, e^{(m_{l-1} - m_l)(x_0 - X_{l-1})}, 1, e^{-(m_l - m_{l-1})(x_0 - X_l)}, \dots), \quad (4.29)$$

where we have defined

$$X_l \equiv -\frac{r_l - r_{l+1}}{m_l - m_{l+1}}, \quad l = 1, \dots, n. \quad (4.30)$$

We denote $\text{Re}(X_l) = x_l$. If we assume

$$x_1 \gg x_2 \gg \dots \gg x_n, \quad (4.31)$$

and consider the region of $x_{l-1} \gg x_0 \gg x_l$, then we see that in (4.29) the l -th flavor component becomes dominant while the other components become negligible:

$$e^{-m_l x_0 - r_l} H_0^{1k} e^{m_k x_0} \sim \delta^{lk}. \quad (4.32)$$

By this way, we can specify the l -th vacuum. Since l runs from 1 to n in this case, it is found that the moduli matrix (4.27) realizes n number of discrete vacua. As x_0 decreases (increases), the dominant element shifts to the right (left) gradually in the flavor space as $\delta^{lk} \rightarrow \delta^{(l-1)k}$ ($\delta^{lk} \rightarrow \delta^{(l+1)k}$). This shift of vacuum from l to $l-1$ occurs around the point x_l . Therefore x_l becomes approximately the position of a domain wall separating the vacua l and $l+1$.⁸

As a slight modification of the above case, it is also possible to take the moduli matrix where there are nonzero components in the second line in (4.27) with zero in the corresponding column components in the first line. For example,

$$H_{0\langle 1 \leftarrow n \rangle} = \begin{pmatrix} \dots & 0 & e^{r_1} & 0 & e^{r_2} & \dots & e^{r_{n-1}} & 0 & \dots \\ \dots & 0 & 0 & e^{r_n} & 0 & \dots & 0 & 0 & \dots \end{pmatrix}. \quad (4.33)$$

⁸For a more detailed discussion of positions of walls, see Appendix A in [5].

This moduli matrix satisfies (4.11). However, a matrix where all elements are nonzero values only for one column, for example,

$$H_{0\langle 1 \leftarrow n \rangle} = \begin{pmatrix} \cdots & 0 & e^{r_1} & e^{r_2} & \cdots & e^{r_{n-1}} & 0 & \cdots \\ \cdots & 0 & e^{r_n} & 0 & \cdots & 0 & 0 & \cdots \end{pmatrix}, \quad (4.34)$$

is not allowed since it does not satisfy (4.11). If there is more than one column where all the components are nonzero values, the situation changes. In other words, $H_0^{1a} \neq 0$ and $H_0^{2a} \neq 0$ with $a = 1, \dots, n$ ($n \geq 2$). As an example, we consider the following moduli matrix

$$H_{0\langle 1 \leftarrow 4 \rangle} = \begin{pmatrix} \cdots & 0 & e^{r_1} & e^{r_2} & 0 & \cdots \\ \cdots & 0 & e^{r_4} & e^{r_3} & 0 & \cdots \end{pmatrix}. \quad (4.35)$$

The constraint (4.11) gives

$$e^{r_1+r_4} + e^{r_2+r_3} = 0. \quad (4.36)$$

There are four exponential factors and therefore it is expected to realize four vacua from this configuration:

$$\begin{aligned} H_{0\langle 1 \rangle} &= \begin{pmatrix} \cdots & 0 & 1 & 0 & 0 & \cdots \\ \cdots & 0 & 0 & 0 & 0 & \cdots \end{pmatrix}, & H_{0\langle 2 \rangle} &= \begin{pmatrix} \cdots & 0 & 0 & 1 & 0 & \cdots \\ \cdots & 0 & 0 & 0 & 0 & \cdots \end{pmatrix}, \\ H_{0\langle 3 \rangle} &= \begin{pmatrix} \cdots & 0 & 0 & 0 & 0 & \cdots \\ \cdots & 0 & 0 & 1 & 0 & \cdots \end{pmatrix}, & H_{0\langle 4 \rangle} &= \begin{pmatrix} \cdots & 0 & 0 & 0 & 0 & \cdots \\ \cdots & 0 & 1 & 0 & 0 & \cdots \end{pmatrix}. \end{aligned} \quad (4.37)$$

However, because of (4.36), only three vacua among them are realized from (4.35). In what follows, we will show this explicitly.

First of all, let us solve the constraint (4.36). For convenience, we introduce the notation $m_3 \equiv -m_2$ and $m_4 \equiv -m_1$, which is consistent with the inequivalent relation $m_A > m_{A+1}$ assumed before. With the use of the relation (4.30), (4.36) is rewritten as

$$e^{(m_1-m_2)X_1} + e^{(m_3-m_4)X_3} = 0. \quad (4.38)$$

It is easily solved by

$$X_1 = X_3 + \frac{i(2n+1)\pi}{m_1-m_2}, \quad n \in \mathbf{Z}. \quad (4.39)$$

It tells us

$$x_1 = x_3. \quad (4.40)$$

Keeping the relation (4.40) in mind, let us read vacua from (4.35). Making the translation (4.17), we have

$$H_{0\langle 1\leftarrow 4 \rangle} \rightarrow \begin{pmatrix} \dots & 0 & e^{m_1 x_0 + r_1} & e^{m_2 x_0 + r_2} & 0 & \dots \\ \dots & 0 & e^{m_4 x_0 + r_4} & e^{m_3 x_0 + r_3} & 0 & \dots \end{pmatrix}. \quad (4.41)$$

Further acting the world-volume symmetry transformation $V = e^{-m_2 x_0 - r_2}$ on (4.41), we have

$$H_{0\langle 1\leftarrow 4 \rangle} \rightarrow \begin{pmatrix} \dots & 0 & e^{(m_1 - m_2)(x_0 - X_1)} & 1 & 0 & \dots \\ \dots & 0 & e^{-(m_2 - m_3)(x_0 - X_2) - (m_3 - m_4)(x_0 - X_3)} & e^{-(m_2 - m_3)(x_0 - X_2)} & 0 & \dots \end{pmatrix}. \quad (4.42)$$

The upper-left and lower-right components are negligible if we consider the region

$$x_1 = x_3 \gg x_0 \gg x_2. \quad (4.43)$$

By using (4.39), the lower-left component is written by

$$-e^{-(m_2 - m_3)(x_0 - X_2) - (m_3 - m_4)(x_0 - X_1)}. \quad (4.44)$$

Though the second term in the exponential is positive under the condition (4.43), this exponential factor can be negligible if x_2 is taken to be small enough. This condition can be still consistent with (4.43). These observations lead to the second vacuum labeled by $\langle 2 \rangle$ in (4.37).

Similarly, we can consider the third vacuum $\langle 3 \rangle$. Multiplying (4.41) by $V = e^{-m_3 x_0 - r_3}$, we have

$$H_{0\langle 1\leftarrow 4 \rangle} \rightarrow \begin{pmatrix} \dots & 0 & e^{(m_1 - m_2)(x_0 - X_1) + (m_2 - m_3)(x_0 - X_2)} & e^{(m_2 - m_3)(x_0 - X_2)} & 0 & \dots \\ \dots & 0 & e^{-(m_3 - m_4)(x_0 - X_3)} & 1 & 0 & \dots \end{pmatrix}. \quad (4.45)$$

The upper-right and lower-left components can be negligible if we consider the following region:

$$x_2 \gg x_0 \gg x_3 = x_1. \quad (4.46)$$

It nevertheless conflicts with the condition (4.43). Therefore, the configuration (4.35) does not give the vacuum $\langle 3 \rangle$ in (4.37) in this case. On the other hand, if (4.46) holds, (4.35) gives the vacuum $\langle 3 \rangle$ while it does not give the vacuum $\langle 2 \rangle$. We have now two possible parameter choices

$$x_1 = x_3 \gg x_2 \gg x_4, \quad (4.47)$$

$$x_2 \gg x_1 = x_3 \gg x_4, \quad (4.48)$$

where the former (latter) leads to vacua in (4.37) except the third (second) one. One can easily check that the first and fourth vacua $\langle 1 \rangle$ and $\langle 4 \rangle$ in (4.37) are obtained from (4.35) with both the choices (4.47) and (4.48). Thus we find that (4.35) represents a double wall interpolating three vacua.

Finally we consider the odd N case. In this case, we have to take into account the scalar H_0^{N+2} . The moduli matrices (4.27) and (4.33) are possible configurations with $H_0^{N+2} = 0$, considering the constraint (4.11), as in the single wall case. The configuration (4.34) is also allowed if $H_0^{N+2} = \sqrt{2}ie^{(r_1+r_n)/2}$.

The configuration (4.41) is also possible, but in this case, (4.41) can give all the vacua (4.37) with some parameter choices satisfying the constraint (4.36) given by

$$2(e^{r_1+r_4} + e^{r_2+r_3}) + (H_0^{N+2})^2 = 0. \quad (4.49)$$

The solution (4.39) is not general any more. We can choose parameters by taking the nonzero value of H_0^{N+2} so that $x_1 \gg x_2 \gg x_3 \gg x_4$, leading to all the vacua (4.37). Thus it is found that (4.35) with nonzero H_0^{N+2} satisfying (4.49) can represent a triple wall interpolating four vacua.

In this section, we have listed various possible forms of moduli matrices. In what follows, by using the results here, we construct an explicit solution for $N \leq 4$ cases and investigate properties of walls.

5 Explicit construction

5.1 $N = 1$ case

In this case, there exist two vacua. The moduli matrix becomes 2-component vectors H_0^α (index a does not run) and one scalar H_0^3 . Here we form them as a 3-component vector, $H_0^i = (H_0^1, H_0^2, H_0^3)$. Moduli matrices exhibiting two vacua are given by

$$H_{0\langle 1 \rangle} = (1, 0, 0), \quad \sigma = -m, \quad (5.1)$$

$$H_{0\langle 2 \rangle} = (0, 1, 0), \quad \sigma = m, \quad (5.2)$$

where m is a mass parameter. They satisfy the constraint (4.11). There should be only one domain wall connecting these two vacua. Let us consider such a configuration. We take a vector with a complex parameter r as

$$H_{0\langle 1 \leftarrow 2 \rangle} = (1, e^r, H_0^3), \quad -\infty < \text{Re}(r) < \infty, \quad (5.3)$$

where we choose the first component as a unit by using the world-volume symmetry transformation (4.6). This configuration describes an elementary wall. The scalar H_0^3 is determined by the constraint (4.11) as

$$H_0^3 = \sqrt{2}ie^{r/2}. \quad (5.4)$$

Repeating the same discussion as in the previous section of a single wall configuration for the odd N case, it is found that the moduli matrix (5.3) gives the first vacuum (5.1) at $x = \infty$ and the second vacuum (5.2) at $x = -\infty$.

Once the moduli matrix H_0 is specified, the BPS wall solution is easily derived. Substituting (5.3) into (4.10), we have

$$S = \sqrt{e^{2mx} + e^{-2mx+2\text{Re}(r)} + 2e^{\text{Re}(r)}}. \quad (5.5)$$

Therefore, from (4.5), we obtain the solution

$$\Phi^1 = \frac{e^{m(x-x_1)}}{\sqrt{e^{2m(x-x_1)} + e^{-2m(x-x_1)} + 2}}, \quad (5.6)$$

$$\Phi^2 = \frac{e^{-m(x-x_1)+i\text{Im}(r)}}{\sqrt{e^{2m(x-x_1)} + e^{-2m(x-x_1)} + 2}}, \quad (5.7)$$

$$\phi^3 = \frac{\sqrt{2}ie^{i\text{Im}(r)/2}}{\sqrt{e^{2m(x-x_1)} + e^{-2m(x-x_1)} + 2}}, \quad (5.8)$$

where $x_1 = \text{Re}(X_1) = -r/m$ as defined in (4.30). The imaginary part of r is a moduli with respect to the broken $SO(2)$ phase. We can also obtain σ through (4.1). Gauging away v_1 from (4.1) by using the $U(1)$ gauge transformation and substituting (5.5) into (4.1), we have

$$\sigma = -\frac{m(e^{2m(x-x_1)} - e^{-2m(x-x_1)})}{e^{2m(x-x_1)} + e^{-2m(x-x_1)} + 2}. \quad (5.9)$$

Plots of these configurations are shown in Fig. 1. The configurations of Φ^1 , Φ^2 and σ form one domain wall solution while ϕ^3 is a solution connecting two trivial vacua. They give the first vacuum (5.1) in the limit $x \rightarrow \infty$ and the second vacuum (5.2) in the limit $x \rightarrow -\infty$. From the plots, it is also seen that x_1 defined by (4.30) is actually the position of the wall.

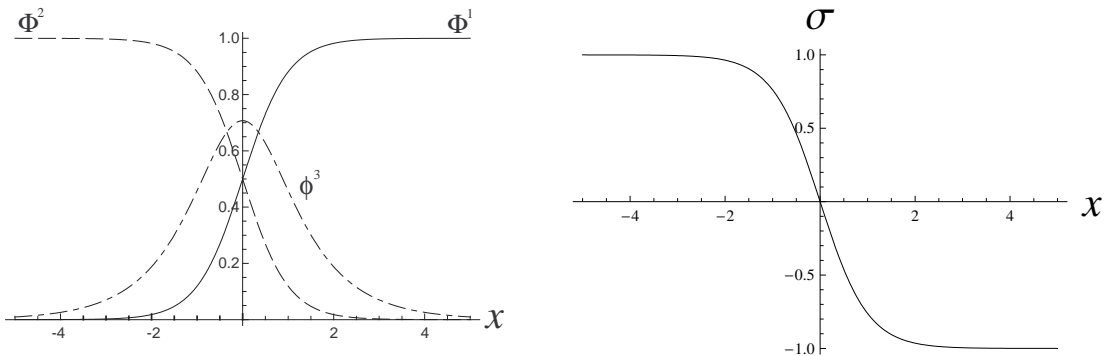


Figure 1: Plots of Φ^1 (solid curve in the left figure), Φ^2 (dashed curve), $\text{Re}(\phi^3)$ (dot-dashed curve) and σ (solid curve in the right figure) with $m = 1$ and $r = 0$.

As we mentioned in the end of Section 2, the number of vacua in the Q^1 case is consistent with the result in the massive NLSM on $T^*\mathbf{C}P^1$. The latter gives one domain wall solution. Therefore, our wall solution is also consistent with this. However, in the Q^1 case, there is also a solution expressed by ϕ^3 in addition to the domain wall solution. This does not exist in the massive NLSM on $T^*\mathbf{C}P^1$ [15]. The difference stems from a different parametrization of the two models. The nonzero solution ϕ^3 is necessary to obtain the wall solution in the Q^1 case.

Vanishing ϕ^3 means that $H_0^3 = 0$ in (5.3). The moduli matrix (5.3) with $H_0^3 = 0$ does not satisfy the constraint (4.11) and it is therefore no longer a solution.

5.2 $N = 2$ cases

In this case, there exist four vacua. Therefore, there should exist richer configurations such as multiwall solutions. The configuration is described by the moduli matrix written by a 2 times 2 matrix $H_0^{\alpha a}$ ($\alpha = 1, 2, a = 1, 2$). Moduli matrices corresponding to four vacua are given by

$$H_{0\langle 1 \rangle} = \begin{pmatrix} 1 & 0 \\ 0 & 0 \end{pmatrix}, \quad H_{0\langle 2 \rangle} = \begin{pmatrix} 0 & 1 \\ 0 & 0 \end{pmatrix}, \quad H_{0\langle 3 \rangle} = \begin{pmatrix} 0 & 0 \\ 0 & 1 \end{pmatrix}, \quad H_{0\langle 4 \rangle} = \begin{pmatrix} 0 & 0 \\ 1 & 0 \end{pmatrix}. \quad (5.10)$$

Single wall configurations are easily obtained, following the classification of single walls in Section 4.2. It is found that there are four possible single wall configurations given by

$$H_{0\langle 1 \leftarrow 2 \rangle} = \begin{pmatrix} 1 & e^r \\ 0 & 0 \end{pmatrix}, \quad H_{0\langle 1 \leftarrow 3 \rangle} = \begin{pmatrix} 1 & 0 \\ 0 & e^r \end{pmatrix}, \quad (5.11)$$

$$H_{0\langle 2 \leftarrow 4 \rangle} = \begin{pmatrix} 0 & 1 \\ e^r & 0 \end{pmatrix}, \quad H_{0\langle 3 \leftarrow 4 \rangle} = \begin{pmatrix} 0 & 0 \\ e^r & 1 \end{pmatrix}, \quad (5.12)$$

where $-\infty < \text{Re}(r) < \infty$. We recognize that they are all elementary walls. These lead to corresponding vacua in (5.10) at boundaries, $x = \pm\infty$. Here we have taken one of the exponential factors to be a unit by using (4.6). Moduli matrices

$$H_{0\langle 1 \leftarrow 4 \rangle} = \begin{pmatrix} 1 & 0 \\ e^r & 0 \end{pmatrix}, \quad H_{0\langle 2 \leftarrow 3 \rangle} = \begin{pmatrix} 0 & 1 \\ 0 & e^r \end{pmatrix}, \quad (5.13)$$

are not allowed since they do not satisfy the constraint (4.11). Explicit solutions for $\Phi^{\alpha a}$ and σ are obtained from (5.11) and (5.12), as obtained in the Q^1 case.

Next we consider a multiwall solution. A possible form of moduli matrix for such a configuration is given by

$$H_{0\langle 1 \leftarrow 4 \rangle} = \begin{pmatrix} e^{r_1} & e^{r_2} \\ e^{r_4} & e^{r_3} \end{pmatrix}, \quad (5.14)$$

where we take $r_1 = 0$ by using (4.6). This is exactly the same case as in (4.35). As we have seen in the discussion below (4.35), (5.14) realizes a double wall configuration interpolating three vacua. This is the multiwall composed of the maximal number of single walls in Q^2 case.

Using the same definition of (4.30), we have two possible parameter choices (4.47) and (4.48). The former choice gives a configuration interpolating the vacua labeled by $\langle 1 \rangle$, $\langle 2 \rangle$ and $\langle 4 \rangle$ and the latter gives one interpolating the vacua labeled by $\langle 1 \rangle$, $\langle 3 \rangle$ and $\langle 4 \rangle$. In order to make clear which vacua are interpolated, in what follows, we shall write these configurations as $H_{0\langle 1\leftarrow 2\leftarrow 4 \rangle}$ and $H_{0\langle 1\leftarrow 3\leftarrow 4 \rangle}$, respectively. An explicit solution is given by

$$\Phi^{\alpha\alpha} = \frac{1}{\left(\sum_{i=1}^4 e^{2m_i x + 2\text{Re}(r_i)}\right)^{1/2}} \begin{pmatrix} e^{m_1 x + r_1} & e^{m_2 x + r_2} \\ e^{m_4 x + r_4} & e^{m_3 x + r_3} \end{pmatrix}, \quad \sigma = -\frac{\sum_{i=1}^4 2m_i e^{2m_i x + 2\text{Re}(r_i)}}{\sum_{i=1}^4 e^{2m_i x + 2\text{Re}(r_i)}}, \quad (5.15)$$

where $m_3 \equiv -m_2$ and $m_4 \equiv -m_1$, and the complex parameter r_i ($i = 1, \dots, 4$) should satisfy the constraint (4.36).

From the double wall configuration one can obtain a single wall configuration (5.11) and (5.12). For instance, taking the limit of $r_3 \rightarrow -\infty$ and $r_4 \rightarrow -\infty$ in (5.14), and using the world-volume symmetry transformation (4.6), it reduces to the single wall configuration $H_{0\langle 1\leftarrow 2 \rangle}$. The constraint (4.11) becomes trivial in this limit. Note that by taking this limit, boundary conditions at $x = \pm\infty$ are changed from $\langle 1 \leftarrow 4 \rangle$ to $\langle 1 \leftarrow 2 \rangle$. The physical meaning of this transition is that one of walls labeled by $\langle 2 \leftarrow 4 \rangle$ in the double wall moves away to infinity along the x direction and the other one labeled by $\langle 1 \leftarrow 2 \rangle$ is left. Similarly, one can recover all the configurations in (5.11) and (5.12) from (5.14).

The double wall configuration (5.15) has another remarkable property. By varying the moduli parameters r_i , the configuration $H_{0\langle 1\leftarrow 2\leftarrow 4 \rangle}$ can be obtained from $H_{0\langle 1\leftarrow 3\leftarrow 4 \rangle}$ and vice versa. Through this transition, a pair of walls in the configuration commutes each other. In Fig. 2, we illustrate this phenomenon. The left figures in Fig. 2 depict the plots of Φ , σ and the tension T for the parameter region (4.47) from top to bottom, corresponding to the configuration $H_{0\langle 1\leftarrow 2\leftarrow 4 \rangle}$. Three vacua $\langle 1 \rangle$, $\langle 2 \rangle$ and $\langle 4 \rangle$ are interpolated by Φ^{11} , Φ^{12} and Φ^{21} with σ . The component Φ^{22} just interpolates trivial vacua at both boundaries and whose absolute value is much less than 1 (see Fig. 3). Two walls approach as r_i varies appropriately and

are located at the same position as $x_1 = x_2 = x_3 > x_4$ (middle figures in Fig. 2). In this parameter region, not only Φ^{22} but also Φ^{12} have absolute values less than 1. It means that the configuration does not interpolate the vacuum $\langle 2 \rangle$ anymore. The components Φ^{11} and Φ^{21} with σ only interpolate the vacua $\langle 1 \rangle$ and $\langle 4 \rangle$ and form a single wall. Taking parameters which satisfy (4.48), the absolute value of Φ^{22} gets increased up to 1 while one of Φ^{12} decreases further (see Fig. 3). As a result, the configuration can interpolate the vacua labeled by $\langle 1 \rangle$, $\langle 3 \rangle$ and $\langle 4 \rangle$ (right figures in Fig. 2). Clearly it corresponds to the configuration $H_{0(1\leftarrow 3\leftarrow 4)}$. Here the signs of Φ^{12} and Φ^{22} flip from the previous two cases, which stem from the solution of the constraint (4.39). Now we have seen that as a pair of walls commutes each other, the intermediate vacua $\langle 2 \rangle$ and $\langle 3 \rangle$ exchange, keeping the vacua at boundaries $\langle 1 \rangle$ and $\langle 4 \rangle$ unchanged. It has been first observed in a SUSY $U(N_C)$ gauge theory which is coupled to N_F massive flavors in the presence of the Fayet-Iliopoulos term with eight supercharges [5]. They are called the penetrable walls. In [5], this phenomenon appears as a non-Abelian nature. (Especially the case for $N_C = 2$ and $N_F = 4$ has been investigated there.) However, here it is found that the penetrable walls are also possible in Abelian case since our model is based on the Abelian gauge theory.

In Fig. 4, we show diagrams representing all possible configurations for Q^2 which consist of single and double wall solutions. It is found that there are four elementary walls and two double walls.

5.3 $N = 3$ case

In this case, the theory has the same number of vacua as the $N = 2$ case. The moduli matrix is also written as the $N = 2$ case, $H_0^{\alpha a}(\alpha = 1, 2, a = 1, 2)$, but there is an additional scalar H_0^5 . Even though there are the same number of vacua as the $N = 2$ case, possible wall configurations are more abundant than the $N = 2$ case. The main reason comes from the difference of the constraint (4.11), in which H_0^5 comes in. Because of this, for instance, there can be a triple wall which is absent in the $N = 2$ case. In the following, we will list possible configurations and discuss properties of solutions.

Moduli matrices representing vacua have the same form with (5.10). The scalar H_0^5 is determined by (4.11), yielding $H_0^5 = 0$.

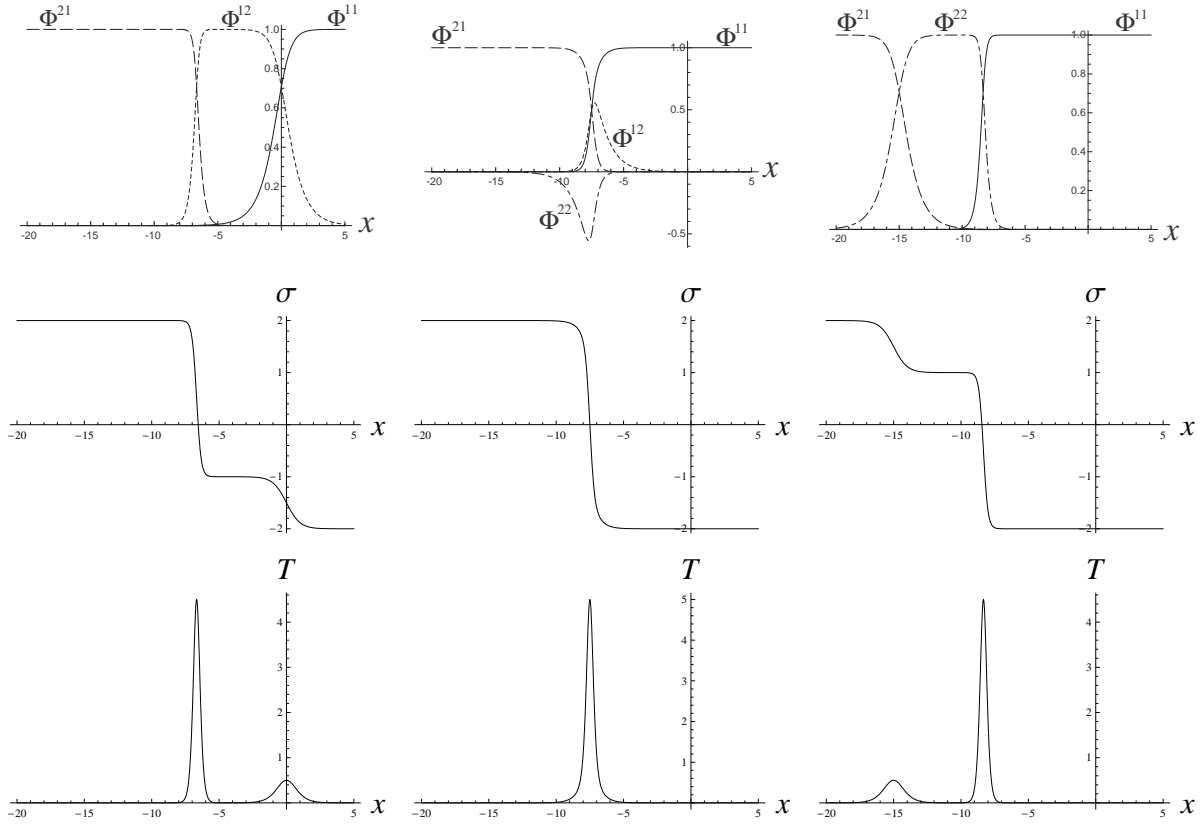


Figure 2: Plots for double wall configurations. The left figures from the top to bottom show plots of Φ , σ and T for the region (4.47) with $r_1 = 0$, $r_2 = 0$, $r_3 = -20$, $r_4 = -20 + i\pi$, respectively. The middle and the right figures show the same plots for the parameter region $x_1 = x_2 = x_3 > x_4$ with $r_1 = 0$, $r_2 = -15/2$, $r_3 = -45/2$, $r_4 = -30$ and (4.48) with $r_1 = 0$, $r_2 = -15$, $r_3 = -25 + i\pi$, $r_4 = -40$, respectively. Solid, dotted, dashed and dot-dashed curves in the top figures depict Φ^{11} , Φ^{12} , Φ^{21} and Φ^{22} , respectively. For all plots we take $m_1 = 2$ and $m_2 = 1$.

Single wall configurations existing in the $N = 2$ case, (5.11) and (5.12), are possible if $H_0^5 = 0$. In addition, as discussed below (4.23), there are two possible single wall configurations

$$H_{0\langle 1\leftarrow 4 \rangle} = \begin{pmatrix} 1 & 0 \\ e^r & 0 \end{pmatrix}, \quad H_0^5 = \sqrt{2}ie^{r/2}, \quad (5.16)$$

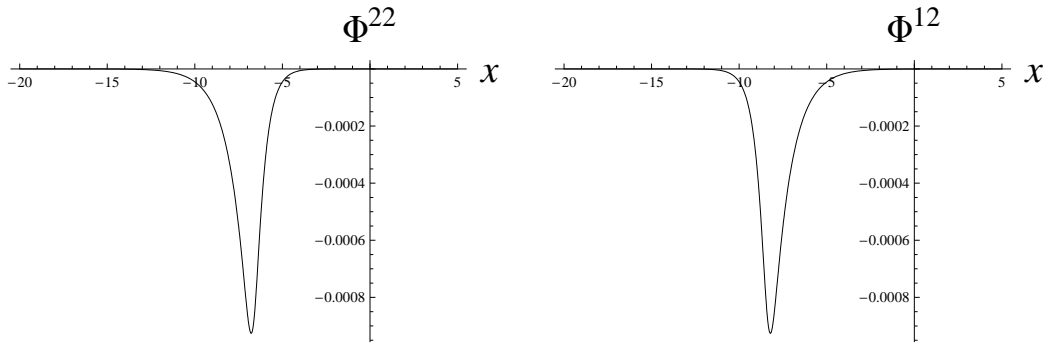


Figure 3: Plots for Φ^{22} and Φ^{12} for the regions (4.47) and (4.48) with the same parameter choices in the left and the right figures in Fig. 2.

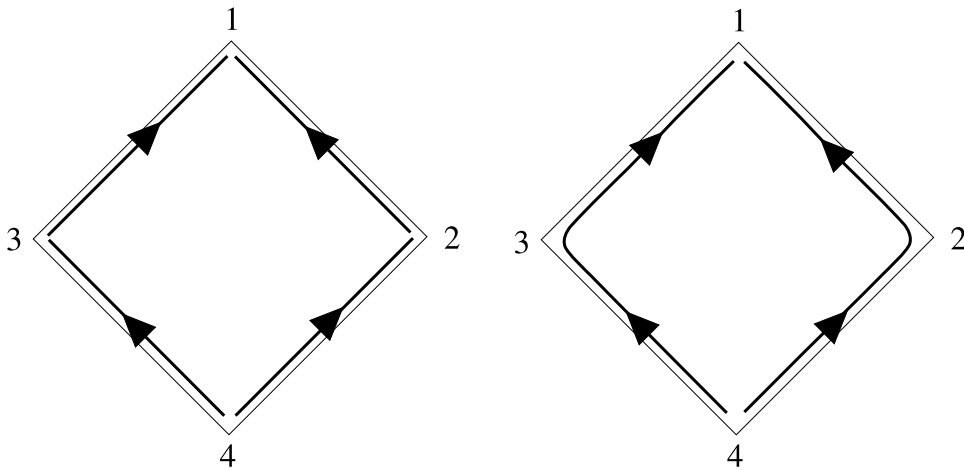


Figure 4: All single (left) and double (right) wall configurations for the Q^2 case. A number labels a vacuum. An arrow with an arrowhead denotes an elementary single wall in the left figure. A single line with two arrowheads denotes a double wall composed of two elementary walls in the right figure.

$$H_{0\langle 2\leftarrow 3 \rangle} = \begin{pmatrix} 0 & 1 \\ 0 & e^r \end{pmatrix}, \quad H_0^5 = \sqrt{2}ie^{r/2}. \quad (5.17)$$

Explicit forms of solutions for $\Phi^{\alpha a}$ and σ are obtained as in the Q^1 case. Putting (5.11), (5.12), (5.16) and (5.17) together, there are six single domain walls (see also the left figure in Fig. 5). Some of them are elementary walls, but the others are compressed walls. The latter does not occur in the $N = 2$ case.

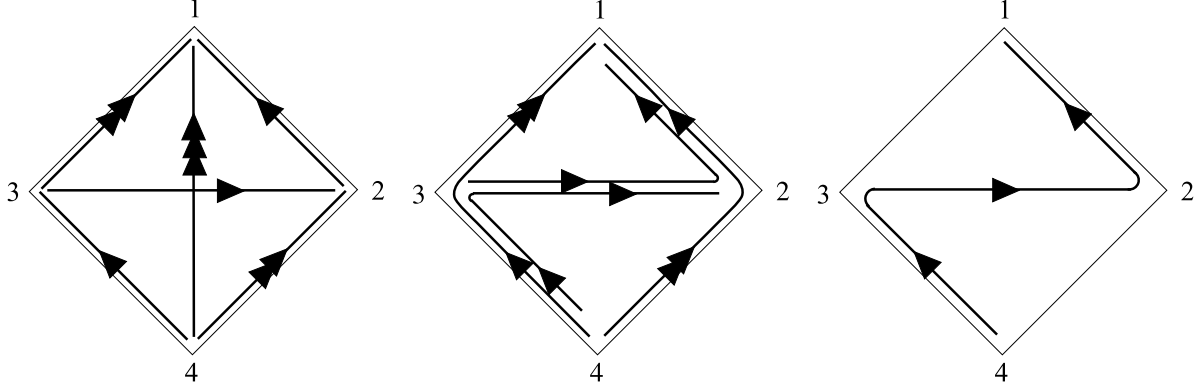


Figure 5: All single (left), double (middle) and triple (right) wall configurations for Q^3 case. An arrow with an arrowhead denotes an elementary single wall and one with a two(three) arrowheads denotes a compressed single wall of level one(two) in the left figure. In the middle figure, there are two double walls composed of two elementary walls and two double walls composed of one elementary wall and one compressed wall of level one. A triple wall in the right figure is composed only by elementary walls.

Let us discuss a double wall configuration. There are two types of moduli matrices to express a double wall configuration. One form is exactly the same as (5.14) in the $N = 2$ case where all components in $H_0^{\alpha a}$ are nonzero values, and the scalar H_0^5 is given by $H_0^5 = 0$. By this setting, all the discussions are the same as in the $N = 2$ case.

Another form is given by $H_0^{\alpha a}$ where there are three nonzero components and the nonzero H_0^5 . The latter is determined by (4.11). Forms of moduli matrices in this case are listed below:

$$H_{0\langle 1\leftarrow 2\leftarrow 3\rangle} = \begin{pmatrix} 1 & e^{r_2} \\ 0 & e^{r_3} \end{pmatrix}, \quad H_0^5 = \sqrt{2}ie^{(r_2+r_3)/2}, \quad (5.18)$$

$$H_{0\langle 2\leftarrow 3\leftarrow 4\rangle} = \begin{pmatrix} 0 & 1 \\ e^{r_4} & e^{r_3} \end{pmatrix}, \quad H_0^5 = \sqrt{2}ie^{r_3/2}, \quad (5.19)$$

$$H_{0\langle 1\leftarrow 2\leftarrow 4\rangle} = \begin{pmatrix} 1 & e^{r_2} \\ e^{r_4} & 0 \end{pmatrix}, \quad H_0^5 = \sqrt{2}ie^{r_4/2}, \quad (5.20)$$

$$H_{0\langle 1\leftarrow 3\leftarrow 4\rangle} = \begin{pmatrix} 1 & 0 \\ e^{r_4} & e^{r_3} \end{pmatrix}, \quad H_0^5 = \sqrt{2}ie^{r_4/2}. \quad (5.21)$$

Here again we take one of the components to be a unit by using (4.6). From these configurations,

we can obtain an elementary wall and a compressed wall. For example, let us consider the configuration (5.18). If one takes the limit of $r_3 \rightarrow -\infty$, the configuration reduces to

$$H_{0\langle 1\leftarrow 2\rangle} = \begin{pmatrix} 1 & e^{r_2} \\ 0 & 0 \end{pmatrix}, \quad H_0^5 = 0. \quad (5.22)$$

The boundary condition changes from $\langle 1 \leftarrow 3 \rangle$ to $\langle 1 \leftarrow 2 \rangle$. It means that by this limit one of walls labeled by $\langle 2 \leftarrow 3 \rangle$ goes away to infinity along the x direction. Therefore, this limit realizes an elementary wall labeled by $\langle 1 \leftarrow 2 \rangle$.

Next we consider another limit. First we multiply (5.18) by $V = e^{-r_2}$ by using the world-volume symmetry transformation (4.6). Then taking the limit of $r_2 \rightarrow \infty$, with keeping the parameter $r_3 - r_2$ finite, we find that (5.18) reduces to the configuration (5.17). In this case, the boundary condition also changes. One of walls goes away to infinity and the rest of the wall becomes an elementary wall labeled by $\langle 2 \leftarrow 3 \rangle$.

Finally let us take the limit of $r_2 \rightarrow -\infty$. The configuration (5.18) becomes

$$H_{0\langle 1\leftarrow 3\rangle} = \begin{pmatrix} 1 & 0 \\ 0 & e^{r_3} \end{pmatrix}, \quad H_0^5 = 0. \quad (5.23)$$

In this limit, the boundary condition does not change unlike the previous two cases. This transition means that two walls approach each other and are compressed to a single wall. Therefore, the configuration (5.23) exhibits a compressed wall. According to the definition below (4.25), this is a compressed wall of level one. This situation is in contrast to the penetrable walls that appeared in the Q^2 case. In that case, a pair of walls just commutes and does not form a compressed wall. A compressed wall here is formed by two elementary walls (5.17) and (5.22). In general, if a single wall is composed as compression of $n + 1$ elementary walls it is called a compressed wall of level n . In Fig. 6, we show an example of a generation of a compressed wall from a double wall configuration, according to this explanation.

Similarly, it can be shown that the configuration (5.19) yields two elementary wall configurations $H_{0\langle 2\leftarrow 3\rangle}$ and $H_{0\langle 3\leftarrow 4\rangle}$ and one compressed wall configuration $H_{0\langle 2\leftarrow 4\rangle}$ by taking some limit of moduli parameters.

Elementary and compressed walls which appear in the above compose other double wall configurations (5.20) and (5.21). For instance, (5.20) is composed of one elementary wall $H_{0\langle 1\leftarrow 2\rangle}$

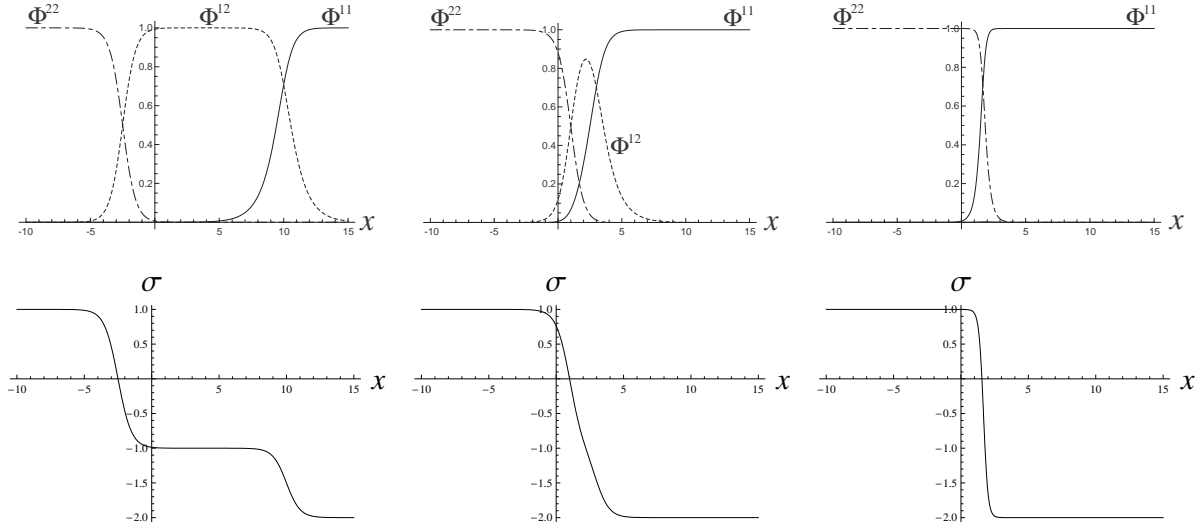


Figure 6: Plots of Φ and σ with $m_1 = 2$, $m_2 = 1$, $r_3 = 5$ and some values of r_2 . The left figure ($r_2 = 10$) shows that there are two separated walls. As r_2 decreases, the left wall approaches the right wall (middle figure, $r_2 = 3$) and eventually both walls are compressed into a single wall (right figure, $r_2 = -4$). Even if r_2 further decreases, a position and a shape of a compressed wall do not change any more.

and one compressed wall $H_{0(2\leftarrow 4)}$. The configurations (5.20) and (5.21) can be compressed into a single wall (5.16) by taking the limit of $r_2 \rightarrow -\infty$ and $r_3 \rightarrow -\infty$, respectively. This single wall (5.16) is compression of three elementary walls and therefore it is a compressed wall of level two.

Finally, we show a triple wall configuration. The corresponding moduli matrix is obtained by taking all components in $H_0^{\alpha a}$ to be nonzero values:

$$H_{0(1\leftarrow 2\leftarrow 3\leftarrow 4)} = \begin{pmatrix} 1 & e^{r_2} \\ e^{r_4} & e^{r_3} \end{pmatrix}, \quad H_0^5 = \sqrt{2}(e^{r_2+r_3} + e^{r_4})^{1/2}, \quad (5.24)$$

where we take one of the factors to be a unit by using (4.6). This triple wall configuration is composed of three elementary walls. Repeating the similar analysis as in a double wall, it is found that (5.24) can be reduced to all the elementary and double walls that have appeared here.

We show the diagrams representing double and triple wall configurations in the middle and

right figures in Fig. 5, respectively. There are four double walls in which two double walls are composed of two elementary walls and the others are composed of one elementary wall and one compressed wall of level one. There is only one triple wall composed by three elementary walls.

5.4 $N = 4$ case

In this case, there are $2[4/2 + 1] = 6$ discrete vacua. As was discussed in Section 2, this result is consistent with one of the massive HK NLSM on $T^*G_{4,2}$. It has been shown that in the latter model there exist six elementary walls, five double walls, two triple walls and one quadruple wall composed of only elementary walls [5]. In this subsection, we will show that our result is consistent with theirs.

In the present case, the moduli matrix is written as a 2 times 3 matrix $H_0^{\alpha a}$ ($\alpha = 1, 2$, $a = 1, 2, 3$). The explicit representation of vacua is given by

$$H_{0\langle 1 \rangle} = \begin{pmatrix} 1 & 0 & 0 \\ 0 & 0 & 0 \end{pmatrix}, \quad H_{0\langle 2 \rangle} = \begin{pmatrix} 0 & 1 & 0 \\ 0 & 0 & 0 \end{pmatrix}, \quad H_{0\langle 3 \rangle} = \begin{pmatrix} 0 & 0 & 1 \\ 0 & 0 & 0 \end{pmatrix}, \quad (5.25)$$

$$H_{0\langle 4 \rangle} = \begin{pmatrix} 0 & 0 & 0 \\ 0 & 0 & 1 \end{pmatrix}, \quad H_{0\langle 5 \rangle} = \begin{pmatrix} 0 & 0 & 0 \\ 0 & 1 & 0 \end{pmatrix}, \quad H_{0\langle 6 \rangle} = \begin{pmatrix} 0 & 0 & 0 \\ 1 & 0 & 0 \end{pmatrix}. \quad (5.26)$$

Six elementary single walls connect two of the vacua as listed below.

$$H_{0\langle 1 \leftarrow 2 \rangle} = \begin{pmatrix} 1 & e^r & 0 \\ 0 & 0 & 0 \end{pmatrix}, \quad H_{0\langle 2 \leftarrow 3 \rangle} = \begin{pmatrix} 0 & 1 & e^r \\ 0 & 0 & 0 \end{pmatrix}, \quad H_{0\langle 2 \leftarrow 4 \rangle} = \begin{pmatrix} 0 & 1 & 0 \\ 0 & 0 & e^r \end{pmatrix}, \quad (5.27)$$

$$H_{0\langle 3 \leftarrow 5 \rangle} = \begin{pmatrix} 0 & 0 & e^r \\ 0 & 1 & 0 \end{pmatrix}, \quad H_{0\langle 4 \leftarrow 5 \rangle} = \begin{pmatrix} 0 & 0 & 0 \\ 0 & e^r & 1 \end{pmatrix}, \quad H_{0\langle 5 \leftarrow 6 \rangle} = \begin{pmatrix} 0 & 0 & 0 \\ e^r & 1 & 0 \end{pmatrix}. \quad (5.28)$$

We show the diagram of possible single wall configurations including elementary and compressed single walls in Fig. 10 in Appendix A.

Next we consider double wall configurations. There are five double walls composed of only elementary walls. Four of them trivially satisfy the constraints (4.11). The moduli matrices are written as

$$H_{0\langle 1 \leftarrow 2 \leftarrow 3 \rangle} = \begin{pmatrix} 1 & e^{r^2} & e^{r^3} \\ 0 & 0 & 0 \end{pmatrix}, \quad H_{0\langle 1 \leftarrow 2 \leftarrow 4 \rangle} = \begin{pmatrix} 1 & e^{r^2} & 0 \\ 0 & 0 & e^{r^4} \end{pmatrix}, \quad (5.29)$$

$$H_{0\langle 3\leftarrow 5\leftarrow 6\rangle} = \begin{pmatrix} 0 & 0 & 1 \\ e^{r_6} & e^{r_5} & 0 \end{pmatrix}, \quad H_{0\langle 4\leftarrow 5\leftarrow 6\rangle} = \begin{pmatrix} 0 & 0 & 0 \\ e^{r_6} & e^{r_5} & 1 \end{pmatrix}. \quad (5.30)$$

The other double wall is given by

$$H_{0\langle 2\leftarrow 5\rangle} = \begin{pmatrix} 0 & 1 & e^{r_3} \\ 0 & e^{r_5} & e^{r_4} \end{pmatrix}, \quad (5.31)$$

with the constraint

$$e^{r_3+r_4} + e^{r_5} = 0. \quad (5.32)$$

This is exactly the same equation as (4.36). Repeating the same analysis below (4.36), for the configuration (5.31) we find two possible parameter regions

$$x_2 = x_4 \gg x_3 \gg x_5, \quad (5.33)$$

$$x_3 \gg x_2 = x_4 \gg x_5, \quad (5.34)$$

where $x_l = \text{Re}(X_l)$ is defined in (4.30) with $r_2 = 0$. The former parametrization excludes the vacuum labeled by $\langle 4 \rangle$ whereas the latter one excludes the vacuum $\langle 3 \rangle$ in the configuration. The moduli matrix (5.31) with the constraint (5.32) therefore connects vacua labeled by $\langle 2 \rangle$, $\langle 3 \rangle$ ($\langle 4 \rangle$) and $\langle 5 \rangle$ under the former (latter) parameter region. A pair of walls in this configuration is a penetrable wall, as we discussed in Section 5.2. In this case, the transition from $H_{0\langle 2\leftarrow 3\leftarrow 5\rangle}$ to $H_{0\langle 2\leftarrow 4\leftarrow 5\rangle}$ (and vice versa) occurs as the positions of two walls exchange. All the double walls composed of only elementary walls for (5.33) and (5.34) are depicted in Fig. 7.

There are two triple walls composed of only elementary walls. The moduli matrices are

$$H_{0\langle 1\leftarrow 5\rangle} = \begin{pmatrix} 1 & e^{r_2} & e^{r_3} \\ 0 & e^{r_5} & e^{r_4} \end{pmatrix}, \quad e^{r_2+r_5} + e^{r_3+r_4} = 0, \quad (5.35)$$

and

$$H_{0\langle 2\leftarrow 6\rangle} = \begin{pmatrix} 0 & 1 & e^{r_3} \\ e^{r_6} & e^{r_5} & e^{r_4} \end{pmatrix}, \quad e^{r_3+r_4} + e^{r_5} = 0. \quad (5.36)$$

Again constraints appeared here are the same form as (5.32). Repeating the same discussion, it is found that the triple wall $H_{0\langle 1\leftarrow 5\rangle}$ connects the vacua labeled by $\langle 1 \rangle$, $\langle 2 \rangle$, $\langle 3 \rangle$ ($\langle 4 \rangle$) and $\langle 5 \rangle$,

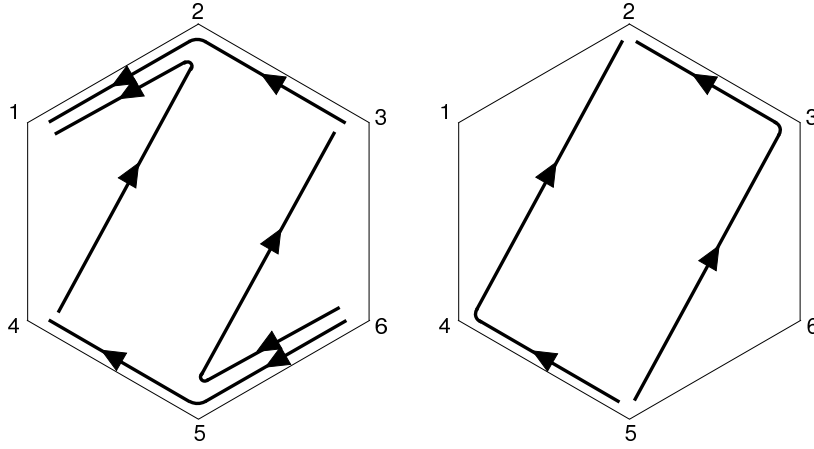


Figure 7: The left figure shows double walls satisfying the constraint (4.11) trivially. The right figure shows a double wall $H_{0\langle 2\leftarrow 5\rangle}$ connecting either the vacuum labeled by $\langle 3\rangle$ or the vacuum labeled by $\langle 4\rangle$. Its explicit interpolation of vacua of $H_{0\langle 2\leftarrow 5\rangle}$ is represented by either $H_{0\langle 2\leftarrow 3\leftarrow 5\rangle}$ or $H_{0\langle 2\leftarrow 4\leftarrow 5\rangle}$.

and $H_{0\langle 2\leftarrow 6\rangle}$ connects the vacua $\langle 2\rangle$, $\langle 3\rangle$ ($\langle 4\rangle$), $\langle 5\rangle$ and $\langle 6\rangle$. These two configurations include penetrable walls. They are single walls labeled by $\langle 2\leftarrow 3\rangle$ ($\langle 2\leftarrow 4\rangle$) and $\langle 3\leftarrow 5\rangle$ ($\langle 4\leftarrow 5\rangle$) for both configurations. The diagrams of the triple walls are given in Fig. 8.

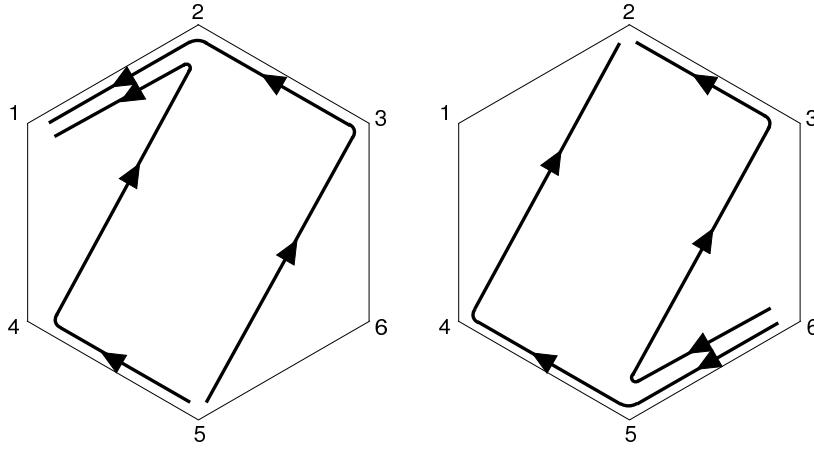


Figure 8: The left figure describes a triple wall $H_{0\langle 1\leftarrow 5\rangle}$, whose explicit interpolation of vacua is represented by either $H_{0\langle 1\leftarrow 2\leftarrow 3\leftarrow 5\rangle}$ or $H_{0\langle 1\leftarrow 2\leftarrow 4\leftarrow 5\rangle}$. The right figure describes a triple wall $H_{0\langle 2\leftarrow 6\rangle}$. Explicit interpolation of vacua is represented by either $H_{0\langle 2\leftarrow 3\leftarrow 5\leftarrow 6\rangle}$ or $H_{0\langle 2\leftarrow 4\leftarrow 5\leftarrow 6\rangle}$.

The moduli matrix for a quadruple wall which is composed of the maximal number of single walls is given by

$$H_{0\langle 1\leftarrow 6 \rangle} = \begin{pmatrix} 1 & e^{r_2} & e^{r_3} \\ e^{r_6} & e^{r_5} & e^{r_4} \end{pmatrix}, \quad (5.37)$$

with the constraint

$$e^{r_2+r_5} + e^{r_3+r_4} + e^{r_6} = 0. \quad (5.38)$$

It interpolates five among six vacua and it is therefore composed of elementary walls only. We will see this in detail below.

First of all let us solve the constraint. The constraint can be solved in the fashion analogous to the previous one. Given the transformation (4.17) and the relation (4.30) with $r_1 = 0$ the constraint (5.38) is written in the form

$$e^{(m_4-m_5)X_4+(m_5-m_6)X_5} + e^{(m_1-m_2)X_1+(m_4-m_5)X_4} + e^{(m_1-m_2)X_1+(m_2-m_3)X_2} = 0, \quad (5.39)$$

where $m_4 = -m_3$, $m_5 = -m_2$ and $m_6 = -m_1$. This can be rewritten as

$$e^{-(m_4-m_5)X_4} = -e^{-(m_2-m_3)X_2} \left[1 + e^{-(m_1-m_2)(X_1-X_5)} \right]. \quad (5.40)$$

Assuming that $x_1 \gg x_5$, the constraint (5.40) can be approximately solved by

$$X_4 \sim X_2 + \frac{i(2n+1)\pi}{m_2-m_3}, \quad n \in Z. \quad (5.41)$$

This tells us that

$$x_2 \sim x_4. \quad (5.42)$$

Taking into account this, we can choose the following parameter regions:

$$x_1 \gg x_2 \sim x_4 \gg x_3 \gg x_5 \gg x_6, \quad (5.43)$$

$$x_1 \gg x_3 \gg x_2 \sim x_4 \gg x_5 \gg x_6. \quad (5.44)$$

The above regions include the same parameter regions with (5.33) and (5.34), respectively. It is therefore found that the moduli matrix (5.37) describes a quadruple wall connecting all the

vacua except either the vacua $\langle 3 \rangle$ or $\langle 4 \rangle$. The quadruple wall includes penetrable walls. They are labeled by $\langle 2 \leftarrow 3 \rangle$ and $\langle 3 \leftarrow 5 \rangle$ for the region (5.43), and $\langle 2 \leftarrow 4 \rangle$ and $\langle 4 \leftarrow 5 \rangle$ for the region (5.44). The diagram of the configurations is illustrated in Fig. 9. For the configuration (5.37), there are other possible parameter choices. They are shown in Appendix B.

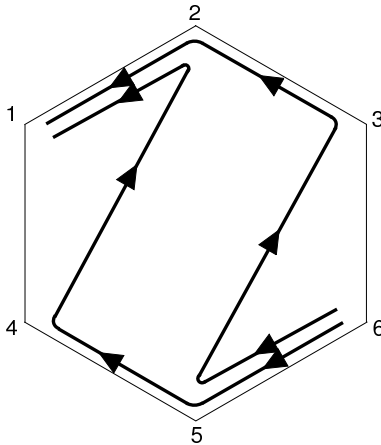


Figure 9: The quadruple wall $H_{0\langle 1 \leftarrow 6 \rangle}$. Explicit interpolation of vacua is represented by either $H_{0\langle 1 \leftarrow 2 \leftarrow 3 \leftarrow 5 \leftarrow 6 \rangle}$ or $H_{0\langle 1 \leftarrow 2 \leftarrow 4 \leftarrow 5 \leftarrow 6 \rangle}$.

Moduli matrices for compressed single walls and multiwalls composed of compressed walls are summarized in Appendix A.

6 Conclusion

We have investigated the vacuum structure and the exact BPS domain wall solutions in the massive Kähler NLSM on the complex quadric surface Q^N . This massive model has been obtained from the massless Kähler NLSM on Q^N in 4-dimensional space-time by the Scherk-Schwarz dimensional reduction. The dimensional reduction gives rise to a nontrivial scalar potential which includes mass terms characterized by the Cartan matrix of $SO(N+2)$. We have assumed generic mass parameters and have found that the theory has $2[N/2+1]$ discrete vacua. The exact BPS multiwall solutions have been derived based on the moduli matrix approach developed in [5, 6], especially for the $N \leq 4$ case. We have also found that the moduli

space of the wall solutions is the complex quadric surface.

We have discussed the consistency of our result with ones previously studied. As mentioned in the Introduction and Section 2, when considering vacua and walls in the massive HK NLSM on $T^*\mathbf{CP}^1$ and $T^*G_{N_F, N_C}$, the cotangent part is irrelevant. We can respect the results in these models as ones in the massive Kähler NLSMs on \mathbf{CP}^1 and G_{N_F, N_C} . For instance, the massive HK NLSM on $T^*\mathbf{CP}^1$ gives two discrete vacua and one domain wall solution interpolating them. Vacua and wall solutions are only described by the \mathbf{CP}^1 part of the model. Since \mathbf{CP}^1 is isomorphic to Q^1 , the same result should be obtained in the Q^1 case. Actually we have found the same number of discrete vacua and domain wall solutions. Similarly, we have checked the consistency for the Q^4 case. This is isomorphic to $G_{4,2}$ and the results of the Q^4 case should be the same with one of the massive HK NLSM on $T^*G_{4,2}$. The latter possesses six discrete vacua and the BPS wall solutions consisting of six elementary single walls, five double walls, two triple walls and one quadruple wall composed of only elementary walls. There also exist single compressed walls and multiwalls including compressed walls. Our wall solutions in the Q^4 case completely coincide with these results.

The results of the Q^2 and Q^3 cases are completely new although there is isomorphism $Q^2 \sim \mathbf{CP}^1 \times \mathbf{CP}^1$ and $Q^3 \sim Sp(2)/U(2)$. It can be guessed that our Q^2 model has four discrete vacua since it consists of two \mathbf{CP}^1 sectors. This has been justified in our analysis. The Q^3 model has a richer structure than the Q^2 model despite the fact that the number of the vacua is the same in both cases. The reason is that the constraint (4.11) is different. The former includes the scalar H_0^{N+2} in (4.11) while the latter does not. When it exists in (4.11), any choice of moduli parameters in $H_0^{\alpha\alpha}$ is possible, since such a choice is compensated by the scalar H_0^{N+2} through (4.11). The same structure is repeated generally for Q^{2n} and Q^{2n+1} ($n \geq 1$). Though both models have the same numbers of discrete vacua $2(n+1)$, since the latter includes H_0^{2n+1} , there are more abundant types of domain wall solutions than the Q^{2n} case. Therefore, the Q^5 model has more kinds of wall solutions than the Q^4 case studied here. Deriving wall solutions in the $N=5$ case is very similar to the $N=3$ case and therefore we do not repeat these here.

We believe that our results obtained in this paper are the same as those of the massive HK NLSM on T^*Q^N for the same reason mentioned above. One way to see is to construct a quotient

action of this model and to derive wall solutions with the help of the moduli matrix approach. However, as we wrote in the Introduction, construction of a quotient action of this model is difficult though its massless version without using a Lagrange multiplier has been constructed [19]. The latter model can be extended into a massive version by using the formulation in [33]. In this formulation, we cannot directly use the moduli matrix approach since it is not written as a gauge theory. It would be interesting to investigate the vacuum structure and wall solutions in this model to check the consistency as a future work.

Acknowledgments

We would like to thank Minoru Eto, Hiroaki Nakajima and Muneto Nitta for discussion. The work of M.A. is supported by the Science Research Center Program of the Korea Science and Engineering Foundation through the Center for Quantum Spacetime (CQUeST) of Sogang University with grant number R11-2005-021. S.L. would like to thank CQUeST for hospitality during this work.

Appendix

A Compressed walls for Q^4

We discuss single walls and multiwalls composed of compressed walls for the $N = 4$ case.

There are four compressed single walls of level one:

$$\begin{aligned} H_{0\langle 1\leftarrow 4 \rangle} &= \begin{pmatrix} 1 & 0 & 0 \\ 0 & 0 & e^r \end{pmatrix}, & H_{0\langle 1\leftarrow 3 \rangle} &= \begin{pmatrix} 1 & 0 & e^r \\ 0 & 0 & 0 \end{pmatrix}, \\ H_{0\langle 4\leftarrow 6 \rangle} &= \begin{pmatrix} 0 & 0 & 0 \\ e^r & 0 & 1 \end{pmatrix}, & H_{0\langle 3\leftarrow 6 \rangle} &= \begin{pmatrix} 0 & 0 & 1 \\ e^r & 0 & 0 \end{pmatrix}. \end{aligned} \tag{A.1}$$

There are two compressed single walls of level two:

$$H_{0\langle 1\leftarrow 5 \rangle} = \begin{pmatrix} 1 & 0 & 0 \\ 0 & e^r & 0 \end{pmatrix}, \quad H_{0\langle 2\leftarrow 6 \rangle} = \begin{pmatrix} 0 & 1 & 0 \\ e^r & 0 & 0 \end{pmatrix}. \tag{A.2}$$

The diagram of the above configurations are depicted in Fig. 10. The compressed single walls can be constructed from the multiwalls as discussed in Section 5.2. It is also read off from this in the diagram in Fig. 10. For instance, it is easy to see that the compressed wall $H_{0\langle 1\leftarrow 4\rangle}$ can be obtained as a compression of the single walls $\langle 1\leftarrow 2\rangle$ and $\langle 2\leftarrow 4\rangle$ in $H_{0\langle 1\leftarrow 2\leftarrow 4\rangle}$ in (5.29).

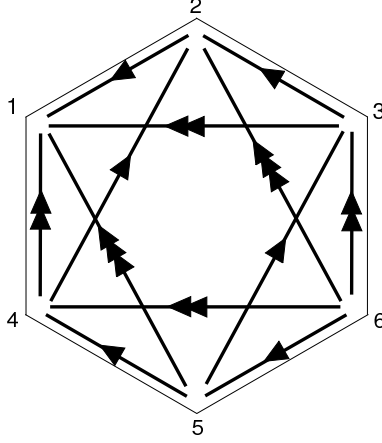


Figure 10: Arrows with one arrowhead denote elementary walls, which are discussed in Section 5.4. Arrows with two arrowheads denote compressed single walls of level one. Arrows with three arrowheads denote compressed single walls of level two. All the arrows point from $x = -\infty$ to $x = \infty$.

There exist four double walls composed of compressed walls of level one:

$$\begin{aligned}
 H_{0\langle 1\leftarrow 3\leftarrow 5\rangle} &= \begin{pmatrix} 1 & 0 & e^{r_3} \\ 0 & e^{r_5} & 0 \end{pmatrix}, & H_{0\langle 1\leftarrow 4\leftarrow 5\rangle} &= \begin{pmatrix} 1 & 0 & 0 \\ 0 & e^{r_5} & e^{r_4} \end{pmatrix}, \\
 H_{0\langle 2\leftarrow 4\leftarrow 6\rangle} &= \begin{pmatrix} 0 & 1 & 0 \\ e^{r_6} & 0 & e^{r_4} \end{pmatrix}, & H_{0\langle 2\leftarrow 3\leftarrow 6\rangle} &= \begin{pmatrix} 0 & 1 & e^{r_3} \\ e^{r_6} & 0 & 0 \end{pmatrix}.
 \end{aligned} \tag{A.3}$$

A double wall

$$H_{0\langle 1\leftarrow 6\rangle} = \begin{pmatrix} 1 & e^{r_2} & 0 \\ e^{r_6} & e^{r_5} & 0 \end{pmatrix}, \quad e^{r_2+r_5} + e^{r_6} = 0, \tag{A.4}$$

is composed of an elementary wall and a compressed wall of level two. Its explicit interpolation

of vacua is represented by either $H_{0\langle 1\leftarrow 2\leftarrow 6\rangle}$ or $H_{0\langle 1\leftarrow 5\leftarrow 6\rangle}$. A double wall

$$H_{0\langle 1\leftarrow 6\rangle} = \begin{pmatrix} 1 & 0 & e^{r_3} \\ e^{r_6} & 0 & e^{r_4} \end{pmatrix}, \quad e^{r_3+r_4} + e^{r_6} = 0, \quad (\text{A.5})$$

is composed of two compressed walls of level two. Its explicit interpolation of vacua is represented by either $H_{0\langle 1\leftarrow 3\leftarrow 6\rangle}$ or $H_{0\langle 1\leftarrow 4\leftarrow 6\rangle}$.

There are two triple walls composed of two elementary walls and a compressed wall of level one:

$$H_{0\langle 1\leftarrow 6\rangle} = \begin{pmatrix} 1 & e^{r_2} & e^{r_3} \\ e^{r_6} & 0 & e^{r_4} \end{pmatrix}, \quad H_{0\langle 1\leftarrow 6\rangle} = \begin{pmatrix} 1 & 0 & e^{r_3} \\ e^{r_6} & e^{r_5} & e^{r_4} \end{pmatrix}. \quad (\text{A.6})$$

Both are constrained by $e^{r_3+r_4} + e^{r_6} = 0$. Explicit interpolation of vacua for the first one is represented by either $H_{0\langle 1\leftarrow 2\leftarrow 3\leftarrow 6\rangle}$ or $H_{0\langle 1\leftarrow 2\leftarrow 4\leftarrow 6\rangle}$. Similarly for the second one it is represented by either $H_{0\langle 1\leftarrow 3\leftarrow 5\leftarrow 6\rangle}$ or $H_{0\langle 1\leftarrow 4\leftarrow 5\leftarrow 6\rangle}$.

B Parameter regions for the configuration (5.37)

In this appendix, we show another choice for parameter regions for the configuration (5.37). Assuming that $x_1 \ll x_5$, the constraint (5.40) leads to $x_2 \ll x_4$. Considering this, possible choices of parameters are in this case, for instance,

$$x_3 \gg x_4 \gg x_5 \gg x_1 \gg x_2 \gg x_6, \quad (\text{B.7})$$

$$x_4 \gg x_5 \gg x_1 \gg x_2 \gg x_3 \gg x_6. \quad (\text{B.8})$$

The parameter choice (B.7) tells us that a quadruple wall configuration interpolates all the vacua except the vacuum $\langle 3\rangle$ since it does not satisfy the condition to lead to this vacuum (see the discussion below (4.43))

$$x_2 \gg x_0 \gg x_3, \quad (\text{B.9})$$

whereas (B.8) excludes the vacuum $\langle 4\rangle$ by the similar reason.

The constraint (5.39) can be also written as

$$e^{(m_5-m_6)X_5} = -e^{(m_1-m_2)X_1} [1 + e^{(m_2-m_3)(X_2-X_4)}]. \quad (\text{B.10})$$

Assuming that $x_2 \gg x_4$ the constraint (B.10) leads to $x_1 \ll x_5$. Possible choices for parameter regions are given by

$$x_5 \gg x_1 \gg x_2 \gg x_3 \gg x_4 \gg x_6, \quad (\text{B.11})$$

$$x_2 \gg x_3 \gg x_4 \gg x_5 \gg x_1 \gg x_6. \quad (\text{B.12})$$

Repeating the same discussion as above, we find that the parameter choices (B.11) and (B.12) represent configurations of quadruple walls interpolating all the vacua except the vacua labeled by $\langle 5 \rangle$ and $\langle 2 \rangle$, respectively.

Finally, if it is assumed that $x_2 \ll x_4$, the constraint (B.10) gives $x_1 \sim x_5$. Appropriate choices for parametrization are

$$x_3 \gg x_4 \gg x_5 \sim x_1 \gg x_2 \gg x_6, \quad (\text{B.13})$$

$$x_4 \gg x_5 \sim x_1 \gg x_2 \gg x_3 \gg x_6. \quad (\text{B.14})$$

In this case, the vacua $\langle 3 \rangle$ and $\langle 4 \rangle$ are not interpolated in the region (B.13) and (B.14), respectively.

References

- [1] E. Witten and D. Olive, *Phys. Lett.* **B78** (1978) 97.
- [2] E. Bogomol'nyi, *Sov. J. Nucl. Phys.* **B24** (1976) 449; M. K. Prasad and C. H. Sommerfield, *Phys. Rev. Lett.* **35** (1975) 760.
- [3] M. Cvetič, F. Quevedo and S. J. Rey, *Phys. Rev. Lett.* **67** (1991) 1836; M. Cvetič, S. Griffies and S. J. Rey, *Nucl. Phys. B* **381** (1992) 301 [arXiv:hep-th/9201007]; M. Cvetič, S. Griffies and H. H. Soleng, *Phys. Rev. D* **48** (1993) 2613 [arXiv:gr-qc/9306005].
- [4] E. R. C. Abraham and P. K. Townsend, *Phys. Lett. B* **291** (1992) 85.

- [5] Y. Isozumi, M. Nitta, K. Ohashi and N. Sakai, Phys. Rev. Lett. **93** (2004) 161601 [arXiv:hep-th/0404198]; Y. Isozumi, M. Nitta, K. Ohashi and N. Sakai, Phys. Rev. D **70** (2004) 125014 [arXiv:hep-th/0405194].
- [6] M. Eto, Y. Isozumi, M. Nitta, K. Ohashi and N. Sakai, J. Phys. A **39** (2006) R315 [arXiv:hep-th/0602170].
- [7] Y. Isozumi, M. Nitta, K. Ohashi and N. Sakai, Phys. Rev. D **71** (2005) 065018 [arXiv:hep-th/0405129].
- [8] M. Eto, Y. Isozumi, M. Nitta, K. Ohashi and N. Sakai, Phys. Rev. D **72** (2005) 085004 [arXiv:hep-th/0506135]; Phys. Lett. B **632** (2006) 384 [arXiv:hep-th/0508241].
- [9] M. Eto, Y. Isozumi, M. Nitta, K. Ohashi and N. Sakai, Phys. Rev. Lett. **96** (2006) 161601 [arXiv:hep-th/0511088]; M. Eto, T. Fujimori, Y. Isozumi, M. Nitta, K. Ohashi, K. Ohta and N. Sakai, Phys. Rev. D **73** (2006) 085008 [arXiv:hep-th/0601181].
- [10] M. Eto, Y. Isozumi, M. Nitta, K. Ohashi and N. Sakai, Phys. Rev. D **72** (2005) 025011 [arXiv:hep-th/0412048].
- [11] M. Eto, M. Nitta, K. Ohashi and D. Tong, Phys. Rev. Lett. **95** (2005) 252003 [arXiv:hep-th/0508130].
- [12] M. Arai, M. Nitta and N. Sakai, Prog. Theor. Phys. **113** (2005) 657 [arXiv:hep-th/0307274].
- [13] J. P. Gauntlett, D. Tong and P. K. Townsend, Phys. Rev. D **63** (2001) 085001 [arXiv:hep-th/0007124].
- [14] J. P. Gauntlett, R. Portugues, D. Tong and P. K. Townsend, Phys. Rev. D **63** (2001) 085002 [arXiv:hep-th/0008221].
- [15] M. Arai, M. Naganuma, M. Nitta and N. Sakai, Nucl. Phys. B **652** (2003) 35 [arXiv:hep-th/0211103].
- [16] M. Arai, E. Ivanov and J. Niederle, Nucl. Phys. B **680** (2004) 23 [arXiv:hep-th/0312037].

- [17] S. J. Gates, Jr. and S. M. Kuzenko, Nucl. Phys. B **543** (1999) 122 [arXiv:hep-th/9810137].
- [18] S. J. Gates, Jr. and S. M. Kuzenko, Fortsch. Phys. **48** (2000) 115 [arXiv:hep-th/9903013].
- [19] M. Arai, S. M. Kuzenko and U. Lindström, JHEP **0702** (2007) 100 [arXiv:hep-th/0612174].
- [20] M. Arai and M. Nitta, Nucl. Phys. B **745** (2006) 208 [arXiv:hep-th/0602277].
- [21] M. Arai, S. M. Kuzenko and U. Lindström, JHEP **0712** (2007) 008 [arXiv:0709.2633 [hep-th]].
- [22] A. Karlhede, U. Lindström and M. Roček, Phys. Lett. B **147** (1984) 297.
- [23] U. Lindström and M. Roček, Commun. Math. Phys. **115** (1988) 21.
- [24] M. Eto, Y. Isozumi, M. Nitta, K. Ohashi, K. Ohta, N. Sakai and Y. Tachikawa, Phys. Rev. D **71** (2005) 105009 [arXiv:hep-th/0503033].
- [25] K. Higashijima and M. Nitta, Prog. Theor. Phys. **103** (2000) 635 [arXiv:hep-th/9911139].
- [26] J. Scherk and J. H. Schwarz, Phys. Lett. B **82** (1979) 60.
- [27] J. Wess and J. Bagger, *Supersymmetry and supergravity*, Princeton, USA: Univ. Pr. (1992).
- [28] E. Calabi and E. Vesentini, Ann. Math. **71**, 472 (1960).
- [29] S. Kobayashi and K. Nomizu, *Foundations of Differential Geometry, Vol. II*, Wiley Interscience, New York (1996).
- [30] L. K. Hua, Ann. Math. **47** (1946) 167.
- [31] L. K. Hua, *Harmonic Analysis of Functions of Several Complex Variables in the Classical Domains*, American Mathematical Society, Providence (1963).
- [32] A. Y. Morozov, A. M. Perelomov and M. A. Shifman, Nucl. Phys. B **248** (1984) 279; A. M. Perelomov, Phys. Rept. **146** (1987) 135.
- [33] S. M. Kuzenko, Phys. Lett. B **638** (2006) 288 [arXiv:hep-th/0602050].